

Article

Genomic and Proteomic Analysis of Six Vi01-like Phages Reveals Wide Host Range and Multiple Tail Spike Proteins

Evan B. Harris , Kenneth K. Ewool , Lucy C. Bowden, Jonatan Fierro, Daniel Johnson, McKay Meinzer, Sadie Tayler and Julianne H. Grose * 

Department of Microbiology and Molecular Biology, Brigham Young University, Provo, UT 84604, USA; harrisevan715@gmail.com (E.B.H.); kewool@student.byu.edu (K.K.E.)

* Correspondence: julianne_grose@byu.edu; Tel.: +1-801-422-4940

Abstract: *Enterobacteriaceae* is a large family of Gram-negative bacteria composed of many pathogens, including *Salmonella* and *Shigella*. Here, we characterize six bacteriophages that infect *Enterobacteriaceae*, which were isolated from wastewater plants in the Wasatch front (Utah, United States). These phages are highly similar to the *Kuttervirus* vB_SenM_Vi01 (Vi01), which was isolated using wastewater from Kiel, Germany. The phages vary little in genome size and are between 157 kb and 164 kb, which is consistent with the sizes of other phages in the Vi01-like phage family. These six phages were characterized through genomic and proteomic comparison, mass spectrometry, and both laboratory and clinical host range studies. While their proteomes are largely unstudied, mass spectrometry analysis confirmed the production of five hypothetical proteins, several of which unveiled a potential operon that suggests a ferritin-mediated entry system on the Vi01-like phage family tail. However, no dependence on this pathway was observed for the single host tested herein. While unable to infect every genus of *Enterobacteriaceae* tested, these phages are extraordinarily broad ranged, with several demonstrating the ability to infect *Salmonella enterica* and *Citrobacter freundii* strains with generally high efficiency, as well as several clinical *Salmonella enterica* isolates, most likely due to their multiple tail fibers.



Citation: Harris, E.B.; Ewool, K.K.K.; Bowden, L.C.; Fierro, J.; Johnson, D.; Meinzer, M.; Tayler, S.; Grose, J.H. Genomic and Proteomic Analysis of Six Vi01-like Phages Reveals Wide Host Range and Multiple Tail Spike Proteins. *Viruses* **2024**, *16*, 289. <https://doi.org/10.3390/v16020289>

Academic Editors: Andreas Kuhn and Julie Thomas

Received: 29 December 2023

Revised: 5 February 2024

Accepted: 7 February 2024

Published: 13 February 2024



Copyright: © 2024 by the authors. Licensee MDPI, Basel, Switzerland. This article is an open access article distributed under the terms and conditions of the Creative Commons Attribution (CC BY) license (<https://creativecommons.org/licenses/by/4.0/>).

Keywords: Vi01; bacteriophage; *Enterobacteriaceae*; tail spike protein; cluster; phage therapy

1. Introduction

Bacteriophages (phages) are the most common and diverse biological entity in the world, with some estimates bringing the number of virions to 10^{31} – 10^{32} [1–4]. Phages have strong antibiotic capabilities, being natural predators of bacteria. During the lytic infection of their host bacteria, phages insert their foreign DNA into the host cell, ending with phage replication and assembly followed by release through cell lysis and death [5,6]. In addition, some phages integrate into the host genome as “temperate” phages and are replicated with the host DNA and thus contribute to host functions and evolution. The abundance of phages, the relative ease of phage discovery, and their clear influence on the evolutionary pathways of bacteria provide great insight into the ecology and evolution of bacteria [7]. This insight is essential to understanding and treating the threat of multidrug resistant bacterial strains [8,9].

Enterobacteriaceae is a large family of Gram-negative bacteria, first classified in the 1930s [10]. It is composed of many pathogens, including *Salmonella*, *Enterobacter*, *Citrobacter*, *Shigella*, *Proteus*, *Serratia*, *Klebsiella*, *Escherichia coli*, and others. They are bacilli, typically between 1–5 μm in length, do not form spores, and may be either motile or nonmotile. They are often normal members of the gut microbiome but pose serious risks when present in other areas of the body. They may cause urinary tract, intestinal, and blood infections [11]. *Enterobacteriaceae* have additionally been frighteningly efficient at developing antibiotic resistance via mutation or plasmid-mediated whole gene acquisition [12]. The American

Journal of Medicine reports that as of 2006, approximately 20% of *Klebsiella pneumoniae* infections and 31% of *Enterobacter* spp. infections in American ICUs are not susceptible to third generation cephalosporins [13]. These numbers have only been increasing in the subsequent years [14,15]. Clearly a deeper understanding of *Enterobacteriaceae* and the phages that infect them is imperative to human health, both to increase the understanding of host evolution and treatment options.

We have recently discovered a total of six *Enterobacteriaceae* phages, namely *Salmonella* typhimurium phages Guerrero, AR2819, FrontPhageNews, SilasIsHot, and Sajous1, as well as one *Shigella* phage ChubbyThor, each of which logged characteristics of the Vi01-like (AKA Viuna-like) phage family (Table 1). This family was proposed in 2010, when *Salmonella* typhimurium-specific phage Vi01 was proposed as a new lineage of Myoviridae [16] and has since been designated as part of the *Ackermannviridae* family by the International Committee on Taxonomy of Viruses (ICTV) [17]. AR2819, FrontPhageNews, ChubbyThor, Sajous1, and SilasIsHot have been previously published in a genome announcement [18] while the isolation, sequencing and initial characterization of Guerrero is described herein. Basic genomic characteristics of these phages can be found in Table 1.

Table 1. Basic genomic characteristics of six Vi01-like phages discovered in the grose lab between 2020 and 2022. The original bacterial host, GenBank accession number, length of genome in base pairs, percent GC composition of the genome, and number of gene products identified are provided.

| Phage Name | Bacterial Host | GenBank Accession # | Genome Length (bp) | GC % | Gene Products |
|----------------|-------------------------------|---------------------|--------------------|-------|---------------|
| AR2819 | <i>Salmonella typhimurium</i> | MW021753 | 156,899 | 44.97 | 223 |
| SilasIsHot | <i>Salmonella typhimurium</i> | MW021760 | 160,559 | 45.13 | 227 |
| Sajous1 | <i>Salmonella typhimurium</i> | MW021757 | 157,255 | 44.86 | 219 |
| FrontPhageNews | <i>Salmonella typhimurium</i> | MW021754 | 157,832 | 44.61 | 220 |
| ChubbyThor | <i>Shigella boydii</i> | OL615013 | 159,319 | 50.1 | 208 |
| Guerrero | <i>Salmonella typhimurium</i> | OP610151 | 157,565 | 44.9 | 215 |

Vi01, like the second phage discovered in this family SboMAG3, was found to be highly specific to its preferred host, which is theorized to be the case due to a virulence capsule antigen-degrading acetyl esterase domain found to be incorporated into one of the phage's three tail spikes [16]. Since 2010, many more phages have been classified as Vi01-like and as of October 2023, we were able to identify a total of 150 Vi01-like phages that infect *Enterobacteriaceae* deposited in NCBI GenBank. Seventy of these Vi01-like phages appear in scientific articles in PubMed, primarily in genome announcements [19–82]. Despite their apparent ease in isolation and widespread nature across several bacterial hosts, few papers have focused on the characterization of these phages (Supplemental Table S1). Herein we present a broad genomic comparison of the phages in this family as well as further characterization of a representative phage through mass spectrometry. In addition, we explore their potential use in phage therapy through host range studies of five of these new phage isolates.

2. Materials and Methods

2.1. Phage Isolation and Host Range

Bacteriophage Guerrero was isolated from wastewater through LB-based enrichment culture grown at 37 °C for 48 h. Bacteria were pelleted by centrifugation and the supernatant was incubated with fresh bacterial overnight for 30 min. and plated for plaques on LB top agar. A single plaque was purified by once again incubating with fresh bacterial

overnight cultures and plating in LB top agar. This single plaque isolation and reinfection was repeated three times. A lysate ($>10^8$ plaque forming units/mL) was made by incubating a plaque from the final purification plate with diluted bacterial overnight in LB. Host range experiments were conducted with high titer lysates ($>10^8$ pfu/mL) and were performed using spot assays to identify positives and negatives, followed by plaque assays to determine efficiency. Briefly, 5 μ L of phage lysate was spotted onto 0.5 mL bacterial overnight that was plated in LB top agar. All negatives were confirmed through three independent high titer spot assays, while any positives were confirmed through efficiency plaque assay in a minimum of two independent assays. Plaque assay consisted of incubating 10-fold dilutions with 0.5 mL of bacteria for 30–45 min, followed by plating in LB top agar.

2.2. Genome Analysis

The Genomic DNA of phage Guerrero was isolated with the Norgen Biotek Phage DNA Isolation Kit (Thorold, ON, Canada) and was prepared for paired-end Illumina HiSeq 2500 sequencing with the New England Biolabs (New England Biolabs, Ipswich, MA, USA) Ultra II DNA kit. Geneious version R.11 [83] was used to assemble the genome, which circularized upon assembly and was subsequently annotated using DNA Master version 5.23.6 [84] and GeneMarkS [85]. All software was used at default settings. The additional genomes included in this study were obtained through NCBI GenBank (see Supplementary Table S1). Whole genome nucleotide dot plots were constructed using Genome Pair Rapid Dotter (Gepard) [86]. A phylogenetic tree was produced using the Mega11 software using the Neighbor-Joining Method [87,88]. The core genome was identified using CoreGenes 3.5 at default settings [89]. Genome homology was visualized using Clinker [90] and Roary [91]. Average Nucleotide Identity (ANI) analysis was performed using FastANI at default settings [92].

2.3. Electron Microscopy

Samples for SEM analysis were prepared by placing 15 μ L of high-titer bacteriophage lysate on a 200-mesh copper carbon type-B electron microscope grid for one–two minutes. The lysate was wicked away and the grids were stained for 2 min using 15 μ L of 2% phosphotungstic acid (pH = 7) or uranyl acetate. Residual liquid was wicked away using Kimtech wipes and the grid was allowed to dry before being imaged. Electron microscopy was performed at Brigham Young University in the Life Sciences Microscopy Lab using a FEI Helios NATOCAB 600i DualBeam FIB/SEM microscope with STEM detector.

2.4. Mass Spectrometry

Two liters of Sajous1 phage lysate were centrifuged at $12,000\times g$ for 15 min at 4 °C. The supernatant was discarded and DNase I and Rnase A were added to the supernatant to a final concentration of 1 μ g/mL each. The phage solution was concentrated by pelleting the phages using a Sorvall GSA centrifuge at $7000\times g$ for 18 h at 4 °C. The phage pellets were resuspended in SM buffer and centrifuged again at $12,000\times g$ for 10 min at 4 °C to remove any remaining cell debris. A CsCl gradient was created using 0.75 g CsCl per ml of phage suspension. Using a Sorvall GSA rotor, the mixture was centrifuged at 25,000 RPM for 24 h at 5 °C. The phage band was pulled and transferred to a dialysis cassette, which was placed in 1 L of gelatin-free SM buffer (50 mM Tris-HCl, 8 mM magnesium sulfate, pH 7.5) containing 1 M NaCl at 4 °C overnight. The cassette was then transferred to 1 L of standard gelatin-free SM buffer (containing 0.1 M NaCl) for 2–3 h at room temperature, which was immediately repeated. The phage was then trypsin digested and prepared for liquid chromatography with tandem mass spectrometry (LC-MS-MS) using Fastprep (MP BioMedicals, Irvine, CA, USA). The spectra identified were mapped back to the genome by BLASTP.

3. Results

3.1. Analysis of Six Vi01-like Phages and Their Relationship to 144 Vi01-like Enterobacteriaceae of the Ackermannviridae

3.1.1. FrontPhageNews, Guerrero, Sajous1, SilasIsHot, AR2819, and ChubbyThor Lie in Two of Five Enterobacteriaceae Ackermannviridae Subclusters

Phages are incredibly diverse and lack a common homologous gene, making a single phylogenetic tree impossible [93]. Because of this, one descriptive way that phages are grouped is phage families called “clusters”. Phages in these families are typically defined as sharing greater than 50% of the homology of their genome, allowing newly discovered phages to be easily classified [94,95]. In order to obtain a full picture of the breadth of the Vi01-like phage cluster first described by Casjens and Grose [4] which are members of the *Ackermannviridae* phage family designated by the ICTV [17], NCBI GenBank was searched for phages with major capsid protein similarity of greater than 80% and as of October 2023, 150 fully sequenced *Enterobacteriaceae* phages were identified as possible cluster members and subsequently confirmed by Gepard dot plot analysis (Supplementary Table S1). Figure 1 contains a Gepard dot plot analysis [86] of 61 representative phages from the 150 identified (the additional phages are highly similar to phages appearing in this dot plot; however, only 61 could be graphed at once). Dot plot comparison reveals five *Enterobacteriaceae Ackermannviridae* subclusters (A, B, C, D, and E) that have similarity over 50% of the genome, with *Salmonella* phages FrontPhageNews, Guerrero, Sajous1, SilasIsHot and AR2819 in cluster A and *Shigella* phage ChubbyThor in cluster B (Figure 1a). This is one additional subcluster from the four reported by Grose and Casjens in 2014 from analysis of only 16 reported Vi01-like *Enterobacteriaceae* phages [4]. Electron microscope analysis of phages Guerrero and AR2819 verified the morphologic resemblance to Vi01-like Myoviridae (Figure 1b,c).

A survey of the relative hosts associated with each subcluster reveals a clear relationship of host with subcluster (Figure 1a) and all six of our phages follow this rule. There are only two exceptions among the 61 analyzed by dot plot where host is not directly correlated with subcluster designation (a single phage exception in subcluster B as well as in subcluster C); however, analysis of all 150 *Enterobacteriaceae Ackermannviridae* gives a clearer picture. Of the 150 phages, subcluster A comprises phages of only *Salmonella* or *E. coli Enterobacteriaceae* hosts (96 phages) and has been designated the *Kuttervirus* genus by the ICTV [17]. In contrast subcluster B contains 16 phages of diverse hosts namely *Salmonella*, *Shigella*, *E. coli* or *Enterobacter* corresponding to the *Agtrevirus* ICTV genus, as well as 16 phages with *Dickeya* hosts that are known as the *Limestonevirus* ICTV genus. This is the one case where our dot plot subcluster analysis differs substantially from the ICTV genus assignments where two ICTV genera exist in one subcluster. Subcluster C (17 total phages corresponding to the ICTV *Taipeivirus* genus) consists of predominantly *Klebsiella* phages and a single *Serratia* phage as well as a single *E. coli* phage, while two *Serratia* phages are the only members of cluster D (known as the *Miltonvirus* ICTV genus). Cluster E contains two *Erwinia* phages and is known as the *Nezavisimistyvirus* ICTV genus. Of note, there are other *Ackermannviridae* genera proposed with only members that infect non-*Enterobacteriaceae* hosts that are not analyzed in this manuscript, namely *Vibrio* phages (the *Vapseptimavirus* and *Kujavirus* ICTV genera) and an *Aeromonas* phage (the *Tedavirus* genus), displaying the wide-spread success of the *Ackermannviridae* phage family. Our subcluster designations are used throughout the remaining manuscript (subclusters A–E).

Measurements were taken of the phages using existing electron microscope images and compared with measurements found in previous studies, where present [20,35,69,73,93,94]. The phages appear to be of a similar size, with reported averages of capsid (85 ± 15 nm) and tail (125 ± 20 nm) within 20% as expected for similar genome size, but tail width (19 ± 5.6 nm) and neck (14 ± 15.5 nm) being more variable as seen in Table 2.

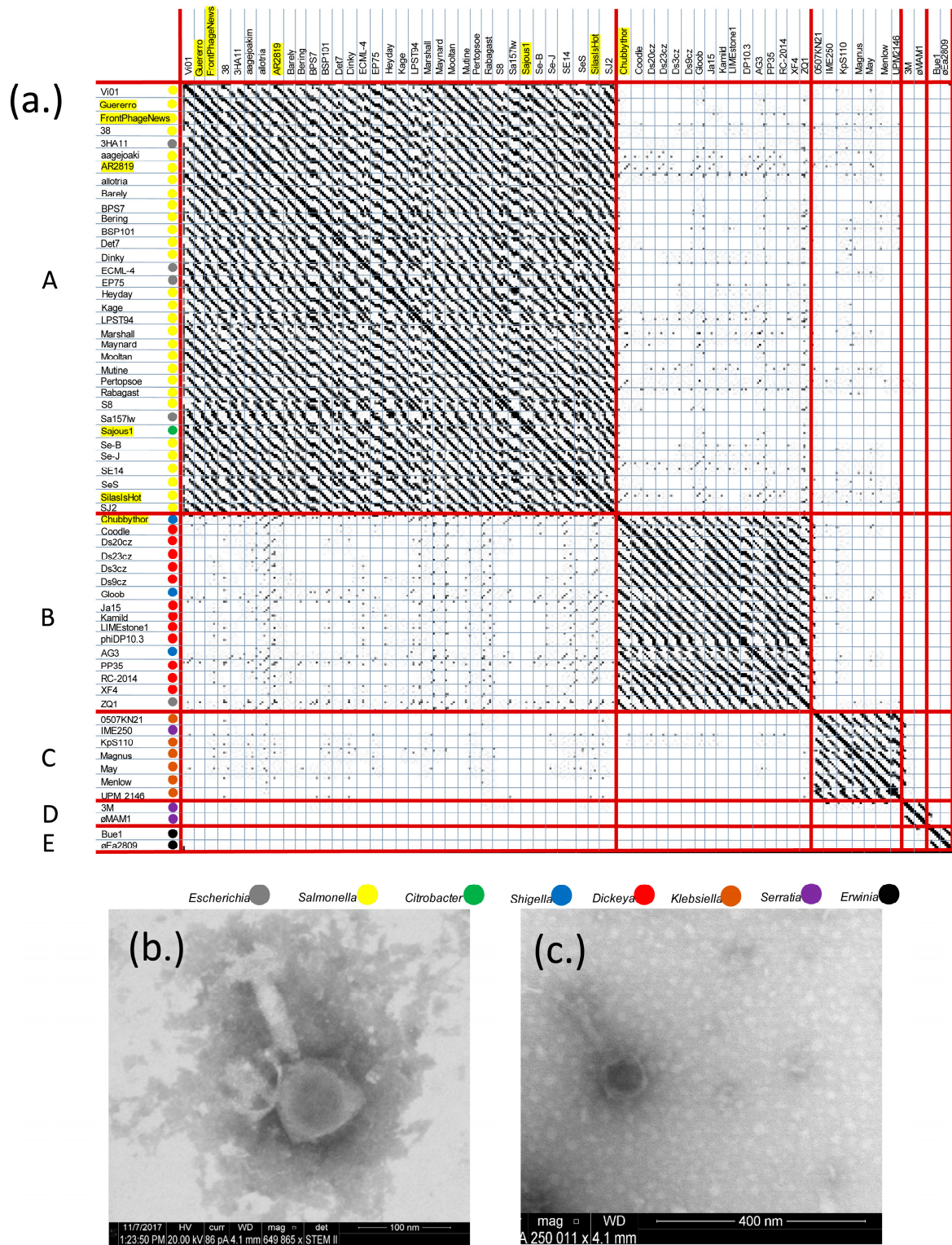


Figure 1. (a) Whole genome dot plot analysis of 61 Vi01-like phages reveals five subclusters of related phages within the *Enterobacteriaceae Ackermannviridae* family, with host (indicated in the colored circles) associating with subcluster designation. Yellow highlighted phages were discovered in our lab. The dot plot was constructed using a locally installed version of Gepard at default settings with whole genome nucleotide sequences as the input files. Default settings are defined in Krumsiek et al., 2007 [86]. (b) Guerrero as imaged by electron microscopy. (c) AR2819 as imaged by electron microscopy.

Table 2. Measurements of select Vi01-like phages. Approximate measurements are provided for representatives from each subcluster. Phages Guerrero and AR2819 were measured using the browser version of program ImageJ 1.54g [95] from electron microscope images in Figure 1b,c, with final measurement composed of the average of three measurements.

| Phage | Cluster | Capsid Diameter | Tail Length | Tail Width | Neck | Reference |
|-------------|---------|-----------------|-------------|------------|-------|------------|
| Vi01 | A | 89 nm | 115 nm | 18 nm | * | [73] |
| Guerrero | A | 103 nm | 118 nm | 23 nm | 10 nm | This study |
| AR2819 | A | 90 nm | 113 nm | 28 nm | ** | This study |
| LIMEstone 1 | B | 91 nm | 114 nm | 17 nm | 20 nm | [20] |
| UPM2146 | C | 51 nm | 173 nm | 10 nm | * | [93] |
| φMAM1 | D | 90 nm | 120 nm | 21 nm | 11 nm | [69] |
| 3M | D | 82 nm | 123 nm | 18 nm | * | [94] |
| Bue1 | E | 79 nm | 126 nm | * | * | [35] |

* Measurements were not provided. ** EM image is not clear enough to provide accurate measurement.

3.1.2. Characteristics of Representative Phages of Vi01-like Subclusters

Due to the high genomic similarity within each subcluster, one phage was selected from each subcluster to be the basis of further genomic comparison: namely Vi01 (A), ChubbyThor (B), Magnus (C), 3M (D), and Bue1 (E) [19,73,94]. A summary of the characteristics of these phages is provided in Table 3.

Table 3. Basic genomic characteristics of a representative genome from each of the Vi01-like *Enterobacteriaceae Ackermannviridae* phage subclusters reported in this manuscript. The genome length (in bp), number of current annotated genes, percent genomic GC content (%GC) (for the purpose of at-a-glance comparison of chemical composition of the representative genomes) and GenBank accession number are provided.

| Phage | Cluster | Length (bp) | # of Genes | %GC | GenBank Accession | Reference |
|------------|---------|-------------|------------|-------|-------------------|--|
| Vi01 | A | 157,061 | 208 | 45.22 | NC_015296 | [73] |
| ChubbyThor | B | 159,319 | 208 | 50.37 | OL615013 | [18] |
| Magnus | C | 157,741 | 217 | 46.26 | MN045230 | [19] |
| 3M | D | 159,398 | 203 | 51.41 | NC_048736 | (Day, Monson and Salmond, unpublished) |
| Bue1 | E | 164,037 | 176 | 50.2 | NC_048702 | [35] |

The average nucleotide identity within subclusters is high (>90%) while the ANI between the five subclusters is 61% and 73% with these representative phages, as seen in Table 4. Subclusters A, B, and C are most similar to one another, with an ANI of ~72%. Subclusters D and E are the most dissimilar, sitting between roughly 61% and 64% similarity to every other subcluster including one another. They stand apart from the high similarity group described above, but also are equally different from one another. This is likely due to their hosts which are *Serratia* and *Erwinia*, which are more dissimilar to all other hosts than are *E. coli*, *Salmonella*, *Shigella* and *Klebsiella*.

Table 4. Average nucleotide identity of one phage from each subcluster of the Vi01-like *Enterobacteriaceae Ackermannviridae*.

| Representative | Cluster | Vi01 | ChubbyThor | Magnus | 3M | Bue1 |
|----------------|---------|--------|------------|--------|--------|--------|
| Vi01 | A | 1 | 0.7287 | 0.7165 | 0.617 | 0.6086 |
| ChubbyThor | B | 0.7287 | 1 | 0.7146 | 0.6353 | 0.6233 |
| Magnus | C | 0.7165 | 0.7146 | 1 | 0.621 | 0.6168 |
| 3M | D | 0.617 | 0.6353 | 0.621 | 1 | 0.633 |
| Bue1 | E | 0.6086 | 0.6233 | 0.6168 | 0.633 | 1 |

A phylogenetic tree was produced using the major capsid protein of 150 of the Vi01-like *Enterobacteriaceae* phages on NCBI [87,96–99]. This is represented in Figure 2, which has been labeled using the subclusters (A–E) identified by the dot plot and ANI analysis above. Phage MCPs appeared to be most similar to orthologous genes in their same subclusters, verifying the subcluster designations made by dot plot and ANI and suggesting little homologous recombination of MCP's between subcluster, perhaps due to the differences between hosts associated with each subcluster [16]. The MCP phylogenetic tree also suggests that the A,B,C evolved from a common progenitor and diverged from D,E, which has a more shallow branch point.

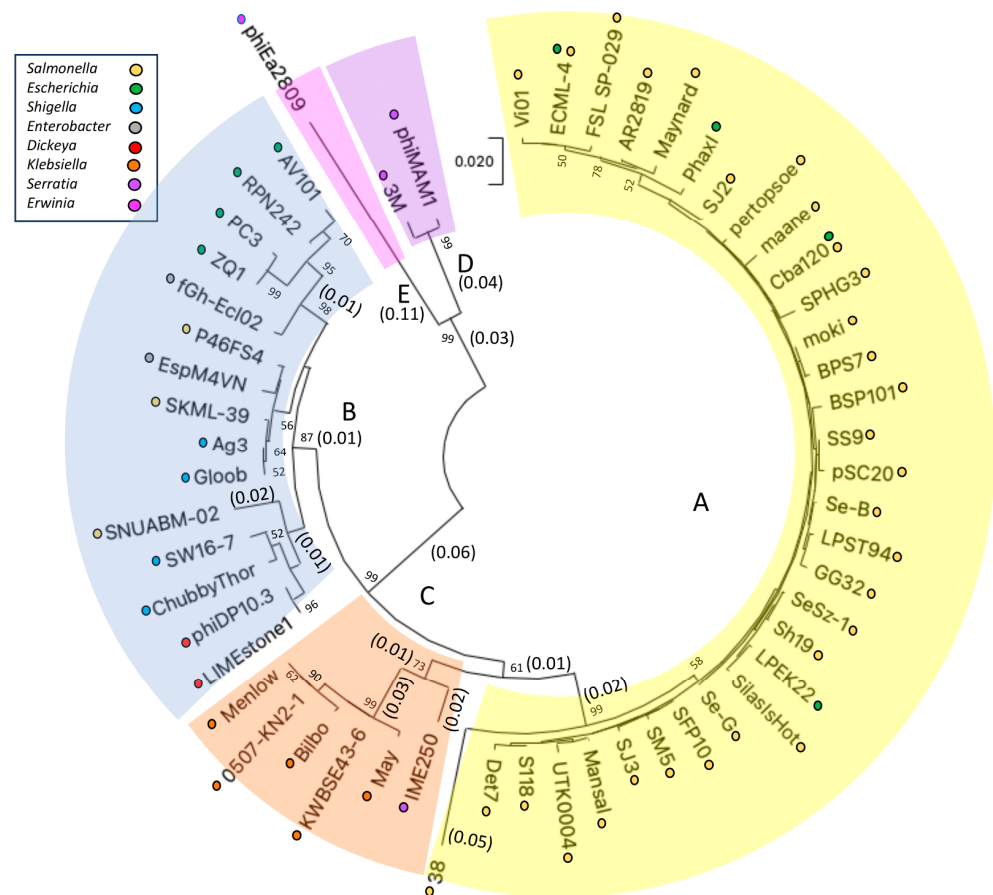


Figure 2. The evolutionary history of 56 unique major capsid proteins (MCPs) identified from 150 *Enterobacteriaceae Ackermannviridae* phages was inferred using the neighbor-joining method [96] and their amino acid sequence. The optimal tree is shown. Phage subcluster designations associated with this manuscript are indicated by branch color and are marked A–E, hosts are indicated by the key, and phages containing identical MCP's are not shown with the complete phage list is available as Supplementary Table S1. The percentage of replicate trees in which the associated taxa clustered together in the bootstrap test (1000 replicates) are shown next to the branches that are >50% (bootstrap tree is not shown) [99]. The tree is drawn to scale, with branch lengths in the same units as those of the evolutionary distances used to infer the phylogenetic tree, with key distances shown in parenthesis as reference. The evolutionary distances were computed using the Poisson correction method [97] and are in the units of the number of amino acid substitutions per site. All ambiguous positions were removed for each sequence pair (pairwise deletion option). There was a total of 447 positions in the final dataset. Original Muscle alignment and subsequent evolutionary analyses were conducted in MEGA11 [87,98].

3.1.3. Analysis of the Conserved Proteins among the Subclusters of the Vi01-like *Enterobacteriaceae*

Using the CoreGenes program at default settings, we were able to identify the core genes present across each of the five subclusters identified above using the one representative from each subcluster along with FrontPhageNews to investigate intra-subcluster relatedness to Vi01 (Table 5) [89]. Phage Vi01 was used as the reference genome in this analysis of six phages in total and 114 core genes were identified. The core genome of the Vi01-like family contains 21 structural protein encoding genes, 41 DNA/RNA-associated protein encoding genes, 3 lysis protein encoding genes, 7 phage assembly protein encoding genes, 3 virulence genes, and 29 hypothetical protein coding genes. In total, the core 114 gene Vi01-like phage genome ranges between 55–67% of the size of the genomes of each phage in the cluster. That is, over half of the genome by gene count is conserved between each representative of each subcluster.

Table 5. Core genome for the *Enterobacteriaceae* Vi01-like *Ackermannviridae* Phages with Vi01 gene products as the reference. Protein types are grouped into assembly, DNA/RNA pathways (DNA/RNA), structural, lysis or virulence-related.

| Function | Type | Vi01 Gene Product # |
|--|------------|---------------------|
| RIIA lysis inhibitor | Lysis | 1 |
| RIIB lysis inhibitor | Lysis | 2 |
| tail fiber | Assembly | 3 |
| putative histone like protein | DNA/RNA | 4 |
| putative topoisomerase II large subunit | DNA/RNA | 5 |
| DNA topoisomerase II small subunit | DNA/RNA | 6 |
| putative tRNA processing enzyme | DNA/RNA | 7 |
| putative ADP-ribose binding protein | DNA/RNA | 8 |
| putative DexA exonuclease | DNA/RNA | 9 |
| dCMP deaminase | DNA/RNA | 10 |
| membrane-flanked domain protein | Virulence | 11 |
| putative head completion protein | Assembly | 12 |
| baseplate tail tube cap | Structural | 13 |
| baseplate wedge subunit | Structural | 14 |
| putative baseplate hub subunit | Structural | 15 |
| putative tape measure protein | Structural | 16 |
| DNA helicase loader | DNA/RNA | 17 |
| putative DNA ligase | DNA/RNA | 18 |
| transcriptional regulator | DNA/RNA | 19 |
| DNA primase-helicase subunit | DNA/RNA | 20 |
| putative RecA protein | DNA/RNA | 21 |
| putative dUTP + B23:B63 diphosphatase | DNA/RNA | 22 |
| putative dNMP kinase | DNA/RNA | 23 |
| putative thymidylate synthase | DNA/RNA | 24 |
| putative thymidylate kinase | DNA/RNA | 25 |
| putative DNA end protector protein | DNA/RNA | 26 |
| putative baseplate tail tube protein | Structural | 27 |
| putative ssDNA binding protein | DNA/RNA | 28 |
| putative late promoter transcription accessory | DNA/RNA | 29 |
| zinc ribbon domain-containing protein | DNA/RNA | 30 |
| RuvC-like Holliday junction resolvase | DNA/RNA | 31 |
| putative baseplate hub subunit | Structural | 32 |
| baseplate hub subunit and tail lysozyme | Structural | 33 |
| baseplate wedge subunit | Structural | 34 |
| Glutaredoxin | DNA/RNA | 35 |
| putative Ribonucleotide-diphosphate reductase beta subunit | DNA/RNA | 36 |
| ribonucleoside-diphosphate reductase subunit alpha | DNA/RNA | 37 |

Table 5. Cont.

| Function | Type | Vi01 Gene Product # |
|--|------------|---------------------|
| PhoH-like phosphate starvation-inducible gene | Virulence | 38 |
| endolysin N-acetylmuramidase | Lysis | 39 |
| putative DNA primase | DNA/RNA | 40 |
| putative adenylosuccinate synthase | DNA/RNA | 41 |
| putative RNA endonuclease | DNA/RNA | 42 |
| putative recombination endonuclease subunit | DNA/RNA | 43 |
| putative recombination/repair endonuclease subunit | DNA/RNA | 44 |
| putative sigma factor for late transcription | DNA/RNA | 45 |
| Ribonuclease | DNA/RNA | 46 |
| putative ATP-dependent helicase | DNA/RNA | 47 |
| putative DNA binding protein | DNA/RNA | 48 |
| Rz-like spanin | Virulence | 49 |
| putative i-spanin | Virulence | 50 |
| putative von Willebrand factor type A domain | Virulence | 51 |
| zinc-finger-containing domain protein | DNA/RNA | 52 |
| nucleoside triphosphate pyrophosphohydrolase | DNA/RNA | 53 |
| RegA-like translation repressor protein | DNA/RNA | 54 |
| putative clamp holder for DNA polymerase | DNA/RNA | 55 |
| putative clamp loader, small subunit | DNA/RNA | 56 |
| putative sliding clamp holder protein | DNA/RNA | 57 |
| DNA helicase | DNA/RNA | 58 |
| Exonuclease | DNA/RNA | 59 |
| UvsY-like recombination mediator | DNA/RNA | 60 |
| putative tail completion protein | Assembly | 61 |
| Major capsid protein | Structural | 62 |
| prohead core scaffold protein | Assembly | 63 |
| head maturation protease | Assembly | 64 |
| putative prohead core protein | Structural | 65 |
| putative portal vertex protein | Structural | 66 |
| putative tail tube protein | Structural | 67 |
| putative tail sheath protein | Structural | 68 |
| terminase large subunit precursor | DNA/RNA | 69 |
| putative terminase small subunit | DNA/RNA | 70 |
| putative proximal tail sheath stabilizer | Assembly | 71 |
| putative neck and head completion protein | Assembly | 72 |
| putative neck protein | Structural | 73 |
| neck protein | Structural | 74 |
| virion structural protein | Structural | 75 |
| putative VrlC protein | Virulence | 76 |
| putative tail fibers protein | Structural | 77 |
| tail spike protein | Structural | 78 |
| putative tail fiber | Structural | 79 |
| baseplate wedge subunit | Structural | 80 |
| baseplate wedge subunit | Structural | 81 |
| putative pyridoxal-phosphate dependent enzyme | DNA/RNA | 82 |
| putative DNA polymerase | DNA/RNA | 83 |
| guanylate kinase | DNA/RNA | 84 |
| guanylate kinase | DNA/RNA | 85 |

These core genes appear to be fairly interspersed throughout the genomes, with structural and assembly genes as well as those involved in DNA/RNA pathways being dispersed throughout the genome. The order of the genes, however, is mostly conserved between the representative phages. There are occasions where gene synteny is broken and genes appear to be randomly distributed throughout the genome as seen in Figure 3. Often, this manifests in small, ~500 bp proteins that, as of yet, have not been defined in any species.

Vi01 gp187, ChubbyThor gp18, Magnus gp20, 3M gp67, and FrontPhageNews gp21 are all highly conserved, though uncharacterized. These gene products are situated roughly 1 kb upstream of a DNA polymerase with the exception of 3M gp67. Rather than sitting just upstream of the DNA polymerase, it can be found 68 kb upstream. This seems to be a result of some type of recombination. Besides a handful of outliers, however, the genomes share a remarkable similarity of genome composition; the structure and placement of genes within the genome is highly conserved between these inter-cluster groups. Among these conserved similarities are important structural proteins like the baseplate hub subunit and portal protein, vital enzymes like endonuclease and primase, RIIA and RIIB lysis inhibitors, and DNA binding proteins like DNA ligase and DNA polymerase clamp loaders.

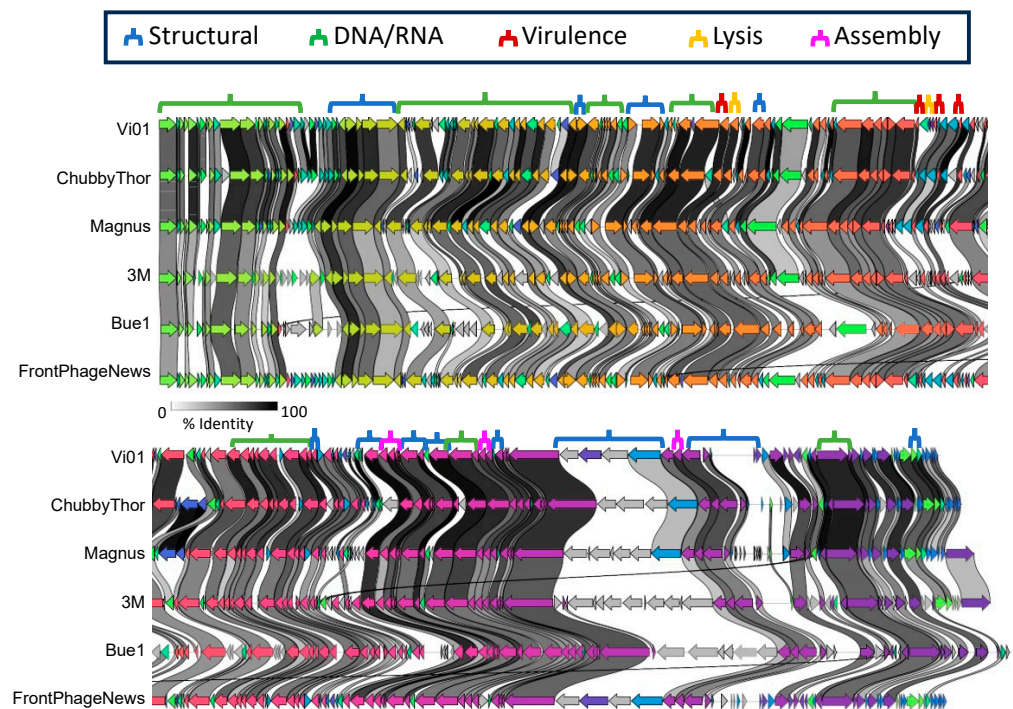


Figure 3. Analysis of the representatives of each Vi01-like *Enterobacteriaceae* subcluster reveals the general homogeneity of their genomes. This figure was made using Clinker [90] at default settings, cut at midpoint, and labeled by hand with identified protein categories. Gene products are indicated by arrows, with direction indicating the encoding strand.

One notable area of difference between the phages is the area beginning between approximately 145 kb and 157 kb which is a segment of the genome that contains structural proteins. Specifically, they are tail proteins. This area contains the least amount of synteny between the phages. Phage tail proteins are one of the main determinants of host specificity, so although the phages are highly conserved this is the area in which we would expect to see the most divergence [100]. This effect is also seen at the structural areas noted at 60 kb and 90 kb, which both code for tail proteins and are also areas of low conservation.

Another notable difference is the presence of nicotinate phosphoribosyl transferase and ribose phosphate pyrophosphokinase, which are important enzymes for the biosynthesis of NAD(+) and phosphoribosyl pyrophosphate, respectively. In the examined phages, these protein-coding sequences were only found in phages ChubbyThor (subcluster B) and Magnus (subcluster C), in which the sequences were highly conserved (97.18% identity) and in the same location (~117.5 kb). These proteins were not found in the other subcluster representatives (even by a tBLASTN search to detect mis-annotation), but an NCBI protein sequence blast revealed these proteins in other cluster B and C phages and also in some phages from cluster A (such as *Salmonella* phage Allotria), whereas Vi01 itself does not encode it, suggesting they were either lost in some members of the subclusters or acquired by others.

3.2. Proteome Characterization of Vi01-like Phages through Structural and Operon Analysis, as Well as Mass Spectrometry

3.2.1. Structural and Operon Analysis of a *Salmonella* phage (FrontPhageNews) of Cluster A and a *Shigella* Phage (ChubbyThor) of Cluster B Provides Putative Functions for 45 Hypothetical Proteins

As it stands, proteomic analysis of most phage contains what has been classified as a large amount of proteomic ‘dark matter’, or proteins with unknown function [101], and the 150 Vi01-like phages analyzed herein are no exception, with most fully annotated phages harboring 50–60% hypothetical or uncharacterized proteins, making further protein analysis imperative in understanding them. Herein the hypothetical and uncharacterized proteins of two phages, a *Shigella* phage (ChubbyThor) of cluster B and a *Salmonella* phage (FrontPhageNews) of cluster A, were analyzed looking for structural homology and putative functions based on protein folding trends, included in Supplementary Table S2. In total, high (>70%)-confidence structural homologs for 37 hypothetical proteins encoded in the genome of FrontPhageNews were found using Phyre2 [102], positing putative functions for these unknown proteins while a total of 26 were found for ChubbyThor. These proteins were then analyzed by HHPRED to check the validity of the results and a majority were supported (Supplementary Table S2). Several of these proteins suggest novel pathways for the Vi01-like phages. Of particular interest, gp98 of FrontPhageNews was found to share 39% structural alignment with the Human C complex spliceosome with a 72.2% confidence, suggesting that RNA splicing could be occurring in this phage and others in the Vi01 family. ChubbyThor’s gp160 shared 26% structural alignment with FtsX with 77.1% confidence. FtsX is a part of the FtsEX complex in *Streptococcus pneumoniae*, a membrane bound complex that transports proteins utilized in cell division [103]. Disruption of the cell division pathways has been previously reported to facilitate phage replication by allowing for cell elongation.

Operon analysis is an additional tool for protein function prediction, in that proteins within an operon usually have related function [104]. Visualized in Figure 4, we identified several likely operons containing proteins of unknown function [105]. Operons were predicted using the Operon-mapper software at default settings [106]. Hypothetical proteins gp173 and 174 from FrontPhageNews are within an operon that includes genes for a translational repressor protein, a DNA polymerase clamp holder, and a clamp loader subunit. These genes could therefore be associated with a DNA polymerase. Given the presence of the repressor gene, they could play a role in inhibiting the synthesis of this polymerase. Gp199 is contained in an operon consisting of genes for head structural proteins and may, therefore, be an additional protein contributing to the structure of the phage capsid. In ChubbyThor, gp43, 44, and 45 are found within an operon containing a transposase, a ribonuclease, and a DNA binding protein, so these may also be involved in transposon activity. Gp67 and 69 are within an operon containing a DNA repair purposed ATPase and a deaminase, so they may also encode DNA repair proteins. Together, structural and operon analysis provide putative functions (or at least pathways) for 45 proteins.

3.2.2. Mass Spectrometry Analysis of Sajous1 Identifies Putative Virion Proteins

Mass spectrometry analysis of cesium chloride (CsCl) purified phage Sajous1 was able to identify spectra corresponding to 31 previously predicted structural proteins, 9 DNA-associated proteins, 2 cell lysis proteins, 5 phage assembly proteins, 6 proteins of miscellaneous function, and 8 hypothetical proteins that are now known to be expressed and are likely part of the virion (Table 6). Gene products 157, 136, 139, 140, and 214 were the top five most highly represented. They were determined to be the major capsid protein, a tail fiber protein, an exo-alpha-sialidase (likely involved in cell wall degradation for phage entry) a putative virulence-associated VriC protein previously associated with host range, and a tail completion protein respectively [47]. Proteins with high counts of retrieved spectra are likely part of the virion, but some with few peptide counts may be contaminants from cellular debris despite purification. However, known virion-associated proteins such as gp142 (a previously reported structural protein) and gp154 (a prohead core protein) also have low peptide counts, making a strict low peptide count unable to distinguish between virion proteins and cell debris contaminants.

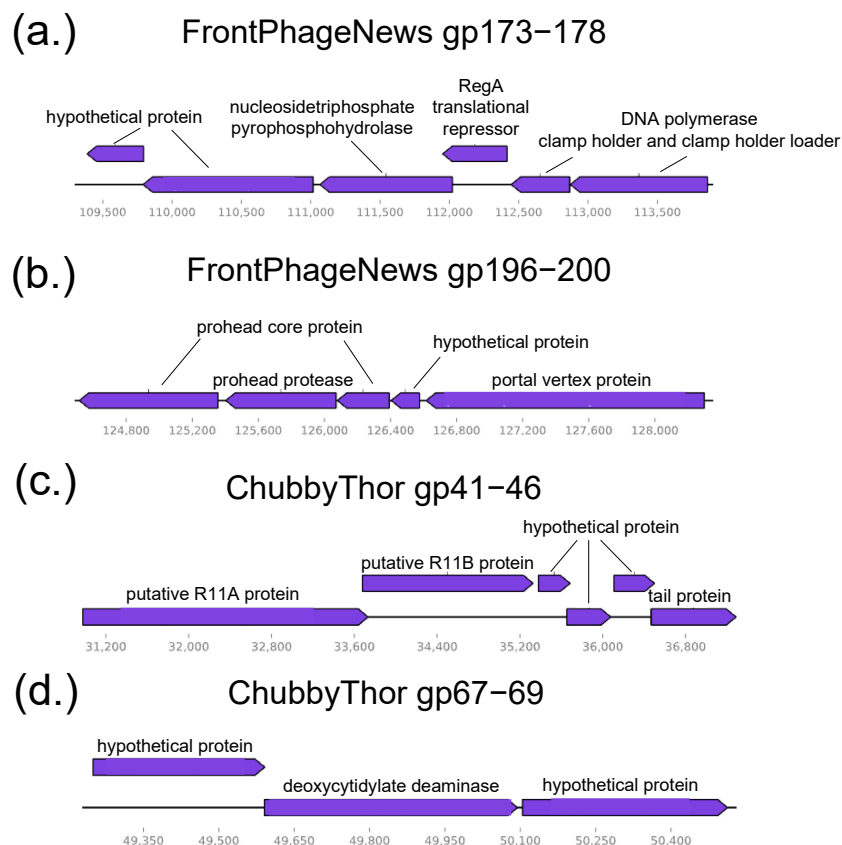


Figure 4. Four operons identified in Vi01-like *Ackermannviridae* phages FrontPhageNews and ChubbyThor suggest putative pathways for protein function. (a) Describes an operon in FrontPhageNews that implies that hypothetical proteins gp173 and 174 are likely involved in DNA polymerase assembly. (b) Describes an operon in FrontPhageNews that indicates that hypothetical protein gp199 is involved in phage head structure. (c) Describes an operon in ChubbyThor that suggests that hypothetical proteins gp43, 44, and 45 are involved in lysis inhibition. (d) Describes an operon in ChubbyThor that indicates that hypothetical proteins gp67 and 69 may encode DNA repair proteins.

Table 6. Mass spectrometry identifies putative components of the Sajous1 virion proteome. Cesium chloride purified virions were subjected to trypsin digest followed by LC/MS/MS. The number of spectra retrieved for each gene product identified is provided along with their annotated functions, with results sorted by function category (phage structural proteins, phage DNA/RNA processes, cell lysis proteins, phage assembly proteins, miscellaneous proteins, and hypothetical proteins of unknown function). Low spectra counts may indicate contamination from cellular proteins. Raw mass spectrometry data is provided as Supplementary Table S3.

| Sajous1 Gene Product | Phage Structural Proteins | # Spectra Retrieved |
|----------------------|--------------------------------------|---------------------|
| gp157 | Major capsid protein | 924 |
| gp136 | Tail fiber protein | 125 |
| gp139 | Exo-alpha-sialidase and tail protein | 113 |
| gp137 | Tail spike protein | 96 |
| gp149 | Tail sheath protein monomer | 89 |
| gp152 | Portal vertex protein of the head | 89 |
| gp138 | Putative tail fiber protein | 89 |
| gp55 | Phage baseplate wedge protein | 80 |
| gp135 | Putative tail fiber protein | 74 |
| gp53 | Putative tape measure protein | 52 |
| gp151 | Tail tube protein monomer | 52 |

Table 6. Cont.

| Sajous1 Gene Product | Phage Structural Proteins | # Spectra Retrieved |
|----------------------|---|---------------------|
| gp83 | Putative tail fiber protein | 43 |
| gp203 | Putative structural protein | 39 |
| gp143 | Putative neck protein | 33 |
| gp115 | Putative structural protein | 31 |
| gp25 | Baseplate tail tube | 24 |
| gp134 | Head closure | 21 |
| gp13 | Tail associated lysozyme | 20 |
| gp56 | T4-like baseplate tail tube cap | 17 |
| gp146 | Proximal tail completion and sheath stabilization | 16 |
| gp119 | Putative tail needle knob | 16 |
| gp145 | Neck and head completion protein | 16 |
| gp54 | Putative baseplate hub subunit | 13 |
| gp55 | Baseplate wedge subunit | 12 |
| gp116 | Phage structural protein | 10 |
| gp166 | Phage putative structural protein | 8 |
| gp168 | Tail completion protein | 8 |
| gp4 | Phage-encoded peptidoglycan binding protein | 6 |
| gp12 | Putative baseplate wedge protein | 6 |
| gp142 | putative virion structural protein | 2 |
| gp154 | Putative prohead core protein | 2 |
| Sajous1 Gene Product | Phage DNA/RNA Processes | # Retrieved |
| gp211 | RegB site-specific RNA endonuclease | 31 |
| gp192 | ParB N-terminal domain containing protein | 11 |
| gp24 | Single-stranded DNA binding protein | 5 |
| gp8 | Glutaredoxin | 4 |
| gp26 | DNA end protector protein | 3 |
| gp179 | Putative DNA-directed RNA polymerase | 3 |
| gp66 | QueC-like queuosine biosynthesis protein | 1 |
| gp31 | Putative thymidylate synthase | 1 |
| gp33 | Putative dUTP diphosphatase | 1 |
| gp174 | Sliding clamp loader | 1 |
| gp180 | Putative DNA-directed RNA polymerase | 1 |
| gp185 | VWA domain-containing protein | 1 |
| Sajous1 Gene Product | Lysis Proteins | # Retrieved |
| gp87 | RIIB protector from prophage-induced early lysis | 2 |
| gp88 | RIIB lysis inhibitor | 1 |
| gp59 | Membrane protein | 1 |
| Sajous1 Gene Product | Phage Assembly Proteins | # Retrieved |
| gp140 | Putative virulence-associated VriC protein | 311 |
| gp214 | Tail completion protein | 196 |
| gp155 | Putative prohead protease | 13 |
| gp156 | Prohead core assembly scaffold | 4 |
| gp148 | Terminase DNA packaging enzyme large subunit | 4 |
| gp147 | Terminase DNA packaging enzyme small subunit | 1 |
| Sajous1 Gene Product | Miscellaneous Functions | # Retrieved |
| gp200 | SPFH domain band 7 family lipoprotein | 3 |
| gp160 | Pyruvate: Ferredoxin oxidoreductase | 1 |
| gp186 | Putative acyl carrier protein | 1 |
| Sajous1 Gene Product | Hypothetical proteins | # Retrieved |
| gp29 | Hypothetical protein | 10 |
| gp120 | Hypothetical protein | 4 |
| gp153 | Hypothetical protein | 2 |
| gp215 | Hypothetical protein | 32 |
| gp216 | Hypothetical protein | 20 |
| gp217 | Hypothetical protein | 10 |

Using Phyre2 analysis, we were able to identify putative structures for the noted hypothetical proteins, shown in Table 7. Gene products 215 and 217 have high confidence values (>60% confidence) for their putative functions, a molybdate binding domain protein and Ferritin, respectively. Gene products 29, 153, and 216 have lower confidence values, but appear to be related to methionine synthase, ATP dependent helicase, and the zeta-subunit of DNA polymerase.

Table 7. Phyre2 analysis of Sajous1 hypothetical proteins identified by mass spectrometry.

| Sajous1 Gene Product | Putative Function | Retrieval # | Confidence | % Identity (% Aligned **) |
|----------------------|---|-------------|------------|---------------------------|
| gp29 | DNA Polymerase zeta-subunit | 10 | 58.2 * | 25 (18) |
| gp120 | Tapasin | 4 | 8.0 * | 40 (59) |
| gp153 | Methionine synthase | 2 | 47.2 * | 13 (82) |
| gp215 | BiMOP duplicated molybdate-binding domain | 32 | 63 | 16 (23) |
| gp216 | ATP-dependent DNA helicase, hydrolase | 20 | 27.3 * | 43 (27.3) |
| gp217 | Ferritin | 10 | 96.7 | 22 (96.7) |

* Low confidence structural alignments ** The % of the original sequence that aligned with the structure of the proposed template.

Combining information gathered from mass spectrometry and comparing it to the putative gene functions identified during annotation, we hypothesize that there may be a polycistronic operon encompassing gene products 214–217. These genes are, respectively, a tail completion protein, a molybdate-binding domain protein, an ATP dependent DNA helicase, and ferritin. It has been proposed that phages may use a strategy called the ‘ferrojan horse’ method of bacterial cell wall attachment for entry [107]. According to this hypothesis, phages hide iron and molybdate ions within tail fibers to try to utilize the bacterial cell’s ion uptake pathways. As these gene products are found in the phage proteome, it is likely that this is a strategy that is in use by the phage.

3.3. Host Range Analysis of Five Enterobacteriaceae Vi01-like Phages

3.3.1. Host Range of Iron-Uptake Mutant Strains and Common Laboratory Enterobacteriaceae

In light of the predicted “ferrojan horse” mode of entry for phage Sajous1, *Salmonella enterica* serovar Typhimurium TonB- and FeoB-deficient strains developed by Tsohis et al. were assessed for phage susceptibility [108]. There are two proteins vital to iron mediated phagocytic infection, TonB and FeoB. FeoB encodes for a homolog of an *E. coli* cytoplasmic membrane iron permease and TonB is an essential element in TonB-dependent siderophore transport. The strains are mutants of *S. enterica* serotype Typhimurium strain IR715 [108,109]. It was found that the five Vi01-like phages had similar infection efficiencies in these mutant strains as compared to the wild-type strains. The data, shown in Table 8, does not appear to suggest the ferrojan horse method to be the only method the phage has for viral infection, at least in the *S. enterica* serovar Typhimurium IR715 host. This suggests that these phages have entry mechanisms that make the proposed ferrojan horse method redundant under laboratory conditions or that they use these anions for some other purpose. This warrants further study of other hosts beyond the scope of this project. The host range analysis of five of the novel Vi01-like phages was also performed on several other common laboratory strains including *S. enterica* serovar Typhimurium, *Citrobacter freundii*, *Cronobacter sakazakii*, *Enterobacter cloacae*, and *Escherichia coli*, *Erwinia amylovora*, *Klebsiella pneumoniae*, *Serratia marcescens*, and *Shigella boydii* (Table 8). In general, the phages were found to have a wide host range capable of infecting multiple genera, with all five tested phages able to infect both *Salmonella typhimurium* and *Citrobacter freundii* lab strains. *Shigella* phage ChubbyThor has the broadest host range in this data, *Shigella boydii* as well as *Salmonella typhimurium* and *Citrobacter freundii*.

Table 8. Vi01-like phage host range efficiency of infection results for TonB -and FeoB-deficient *Salmonella* as well as common laboratory *Enterobacteriaceae* strains. All plaque assays were reproducible and were verified in at least two independent experiments with averages provided. ND is no infection detected.

| Bacteria Name | AR2819 | FrontPhage-News | SilasIsHot | Sajous1 | ChubbyThor |
|---|----------------------|----------------------|----------------------|----------------------|----------------------|
| WT <i>Salmonella enterica</i> IR715 | 1.5×10^{10} | 8.0×10^{10} | 6.9×10^{10} | 8.1×10^{10} | 5.4×10^{13} |
| <i>tonB Salmonella</i> IR715 | 1.8×10^9 | 7.9×10^{10} | 6.6×10^{10} | 7.2×10^{10} | 4.9×10^{13} |
| <i>feoB Salmonella</i> IR715 | 1.5×10^9 | 5.8×10^{10} | 8.1×10^9 | 8.9×10^9 | 8.4×10^{12} |
| <i>tonB feoB Salmonella</i> IR715 | 1.6×10^{10} | 9.0×10^{10} | 5.9×10^{10} | 8.4×10^{10} | 5.3×10^{13} |
| <i>Salmonella</i> Typhimurium LT2 | 3.4×10^{11} | 2.0×10^{10} | 2.6×10^{10} | 6.0×10^{10} | 4.7×10^{10} |
| <i>Citrobacter freundii</i> ATCC 8090 | 1.6×10^{10} | 6.0×10^9 | 2.0×10^9 | 3.4×10^8 | 1.7×10^9 |
| <i>Cronobacter sakazakii</i> ATCC 29544 | ND | ND | ND | ND | ND |
| <i>Enterobacter cloacae</i> ATCC 13047 | ND | ND | ND | ND | ND |
| <i>Escherichia coli</i> K12 | ND | ND | ND | 1.2×10^8 | * |
| <i>Erwinia amylovora</i> ATCC 29780 | ND | ND | ND | ND | ND |
| <i>Serratia marcescens</i> ATCC 27143 | ND | ND | ND | ND | ND |
| <i>Shigella boydii</i> ATCC 9207 | ND | ND | ND | ND | 7.2×10^{11} |
| <i>Klebsiella pneumoniae</i> ATCC 10031 | ND | ND | ND | ND | ND |

* A very clear plaque was observed by spot assay only with the concentrated lysate, indicating possible infection-independent lysis.

3.3.2. Host Range of Clinical *Enterobacteriaceae* Isolates

The five phages were also tested for their ability to infect clinically relevant *Enterobacteriaceae* strains (Table 9). Isolates 0031 and 0409, both *S. enterica* serovar Typhimurium strains, showed plaques from all five phages with *Shigella* phage ChubbyThor displaying reduced efficiency on 0031. Isolate 0404, a *Salmonella heidelberg* strain, showed plaques when combined with every phage excluding FrontPhageNews, while ChubbyThor showed a 10,000-fold reduction on this *Salmonella* strain compared to 0409. *Shigella sonnei* isolates 0422 and 0426 each showed plaques with one phage, Sajous1. In both instances, infection occurred at a reduced efficiency (an approximately 1-million-fold reduction), suggesting these may be mutant phages of some sort. Although Sajous1 was the only phage capable of infecting *E. coli* in laboratory strain culture, our clinical O157:H7 *E. coli* isolates showed plaques when introduced to Sajous1, AR2819, and FrontPhageNews. These results are generally consistent with the host infection efficacies in the nonclinical strains (Table 8) and suggest these phages may be useful in a clinical setting. We see high counts of plaque forming units across the board in *S. enterica* serovar Typhimurium strains. This seems to indicate that amongst the strains of *S. enterica* tested, phage titer concentrations were not affected by the antibacterial resistance mechanisms present in the clinical strains.

Table 9. Host range titer results on clinical isolates suggests possible *Salmonella* phage therapy application for Vi01-like phages. Strain *Salmonella enterica* LT2 titer was performed as a reference for the *Escherichia coli* isolates which were assayed on a separate date. All plaque assays were reproducible and were verified in at least two independent experiments with averages provided. ND is no infection detected.

| Bacterium * | Strain | AR2819 | Front-PhageNews | SilasIsHot | Sajous1 | Chubby-Thor |
|------------------------------|--------|----------------------|----------------------|-----------------------|----------------------|--------------------|
| <i>Salmonella enterica</i> | #0031 | 3.1×10^{12} | 1.6×10^{12} | 1.0×10^{12} | 1.5×10^{11} | 7.6×10^4 |
| <i>Salmonella enterica</i> | #0409 | 2.5×10^{12} | 2.7×10^8 | 1.1×10^8 | 3.1×10^{11} | 1.2×10^9 |
| <i>Salmonella heidelberg</i> | #0404 | 2.4×10^{12} | ND | 1.80×10^{11} | 3.1×10^{12} | 1.12×10^5 |
| <i>Salmonella albert</i> | #0401 | ND | ND | ND | ND | ND |
| <i>Salmonella cubana</i> | #0402 | ND | ND | ND | ND | ND |
| <i>Salmonella infantis</i> | #0410 | ND | ND | ND | ND | ND |

Table 9. Cont.

| Bacterium * | Strain | AR2819 | Front-PhageNews | SilasIsHot | Sajous1 | Chubby-Thor |
|---------------------------------|--------|----------------------|----------------------|----------------------|-------------------|----------------------|
| <i>Salmonella senftenberg</i> | #0405 | ND | ND | ND | ND | ND |
| <i>Salmonella corvallis</i> | #0406 | ND | ND | ND | ND | ND |
| <i>Shigella flexneri</i> | #0421 | ND | ND | ND | ND | ND |
| <i>Shigella flexneri</i> | #0423 | ND | ND | ND | ND | ND |
| <i>Shigella flexneri</i> | #0424 | ND | ND | ND | ND | ND |
| <i>Shigella flexneri</i> | #0425 | ND | ND | ND | ND | ND |
| <i>Shigella sonnei</i> | #0030 | ND | ND | ND | ND | ND |
| <i>Shigella sonnei</i> | #0422 | ND | ND | ND | 1.6×10^6 | ND |
| <i>Shigella sonnei</i> | #0426 | ND | ND | ND | 8.7×10^5 | ND |
| <i>Citrobacter freundii</i> | #0021 | ND | ND | ND | ND | ND |
| <i>Citrobacter freundii</i> | #0023 | ND | ND | ND | ND | ND |
| <i>Citrobacter freundii</i> | #0022 | ND | ND | ND | ND | ND |
| <i>Citrobacter koseri</i> | #0024 | ND | ND | ND | ND | ND |
| <i>Citrobacter koseri</i> | #0025 | ND | ND | ND | ND | ND |
| <i>Salmonella enterica</i> | LT2 | 1.1×10^{11} | 3.4×10^{10} | 5.4×10^{10} | 8.8×10^8 | 3.3×10^7 |
| <i>Escherichia coli</i> O157:H7 | 300748 | 3.6×10^{10} | 1.7×10^9 | ND | 7.0×10^3 | 1.5×10^9 |
| <i>Escherichia coli</i> O157:H7 | 300598 | 1.7×10^{11} | 1.3×10^{10} | ND | 1.4×10^7 | 8.0×10^9 |
| <i>Escherichia coli</i> O157:H7 | 298559 | 2.6×10^{10} | 4.0×10^9 | ND | 1.5×10^8 | 2.1×10^{10} |
| <i>Escherichia coli</i> O157:H7 | 298521 | 3.7×10^{11} | 2.0×10^{10} | ND | 3.5×10^8 | 9.4×10^8 |
| <i>Escherichia coli</i> O157:H7 | 290116 | 8.0×10^9 | 1.2×10^{10} | ND | 2.4×10^7 | 4.7×10^{10} |

* Bacterial *Salmonella*, *Shigella* and *Citrobacter* isolates were obtained from the Center for Disease Control and are summarized in Supplementary Table S4, while *Escherichia coli* O157:H7 were obtained from IHC.

3.3.3. Tail Spike Protein Analysis Reveals Four Tail Spike Proteins in Five *Enterobacteriaceae* Vi01-like Phages That May Explain Their Broad Host Range

Recently Sorensen et al. performed an in-silico analysis of 99 *Ackermannviridae* family phages tail spike proteins that suggested a direct correlation with genera (much like the MCP analysis presented in Figure 2) [47]. They found that most *Ackermannviridae* encoded up to four tail spike proteins that fall into four distinct types, which they termed TSP1-TSP4 with several subtypes. The tail spike genes are generally flanked by the conserved virulence associated gene (*vriC*) and a baseplate wedge gene. Sorenson et al. also identified a conserved motif (GTTAVSL) in TSP1, TSP3 and TSP4 of *Kuttervirus* phages that may allow recombination and hence host specificity alterations. A similar comparison of the tail spike proteins of the six phages reported herein is provided in Table 10.

Salmonella phages AR2819, FrontPhageNews, Guerrero, SilasIsHot, and Sajous1 each encoded a recognizable TSP1, TSP2, TSP3 and TSP4 that was most closely related to TSPs in the genera to which they belong (the *Kutterviridae*), consistent with the findings of Sorensen et al. (Table 10). However, the only two phages to display the same TSP1 through TSP4 subtypes were Guerrero and Sajous1. Analysis of TSP1 revealed that all four *Salmonella* phages AR2819, FrontPhageNews, Guerrero, Sajous1 and *Shigella* phage ChubbyThor share a TSP1-2 tail fiber, while *Salmonella* phage SilasIsHot has a unique TSP1-18. Analysis of TSP2 revealed that SilasIsHot also contains a unique TSP2. Little is known about the TSP2-5 subtype of SilasIsHot, while the TSP2-1 subtype, which the rest of the phages harbor, has recently been shown to contribute to off-target *Citrobacter* recognition by Gil et al., explaining our *Citrobacter* host range results in Table 9 [110]. In addition, TSP2-1 is known to bind and degrade the O:157O-antigen on Shiga toxin (Stx) producing *E. coli*, which hinted at their ability to infect the O157:H7 clinical strains [111]. Clinical O157:H7 strains were therefore acquired and tested (Table 9). As predicted, only SilasIsHot was unable to infect the O157:H7 isolates. Sajous1 displayed a reproducible reduced efficiency on O157:H7 for unknown reasons (perhaps due to variation in other tail spike proteins or variation in TSP2-1). Analysis of TSP3 revealed all five *Salmonella* phages contain TSP3-1 which is predicted to recognize *S. enterica* serovars including *S. Typhimurium*, *S. Derby*, *S. 4.12:i:-*, *S. 4.5.12:1:*, *S. enteritidis*, and *S. Goettingen* O:4 and O9, explaining why *Salmonella*

is a common host [48,110]. Analysis of the final tail fiber, TSP4, revealed FrontPhageNews contains a unique TSP4 among these six phages, which could explain its inability to infect *S. Heidelberg*; however, TSP4-2 has been suggested to recognize *E. coli* O:78 [49].

Conserved *Shigella* phage ChubbyThor encodes three (not four) recognizable tail fibers that were most closely related to those of other *Agtreviridae* (primarily *Shigella* phage AG3 and *Salmonella* phage P46FS4), including two TSP1 proteins and no recognizable TSP3, even when the AG3 TSP3 was used to search the ChubbyThor genome by NCBI's TBLASTN.

Table 10. Analysis of tail spike proteins (TSP) of phages AR2819, FrontPhageNews, Guerrero, SilasIsHot, Sajous1 and ChubbyThor. Phage tail fibers were analyzed and classified according to the designations of Sorensen et al. [49]. The phage gene product number is provided, followed by TSP subtype with the phage and its protein used to determine subtype in parenthesis. Subtype hosts and accession numbers are *Escherichia* phage ECML-4 gp89(AFO10352.1) and 190(AFO10351.1), *Salmonella* phage Moolton gp44(AXY85148.1), *Salmonella* phage Maynard gp38 (AGY47760.1), *Escherichia* phage CBA120 gp213(AEM91899.1), *Salmonella* phage Barely orf5 (QIG62071.1), *Salmonella* phage P46FS4 orf5 (QIG62071.1), *Escherichia* phage SA157IWgp4 (AXF39258.1), *Salmonella* phage SFP10 gp161(AEN94256.1), *Salmonella* phage DET7 gp 206 (YP_009140378.1), *Shigella* phage AG3 bp207(YP_003358662.1) and 213(YP_003358665.1).

| TSP | AR2819 | Front-PhageNews | Guerrero | SilasIsHot | Sajous1 | ChubbyThor |
|------|---------------------------------------|--|--|---------------------------------------|--|---|
| TSP1 | gp56 TSP1-20 (ECML-4, gp189) | gp214 TSP1-20 (ECML-4, gp189) | gp170 TSP1-20 (ECML-4, gp189) | gp221 TSP1-18 (SA157IW, gp4) | gp139 TSP1-20 (ECML-4, gp189) | gp207 TSP1-24 (AG3, gp207) gp208 TSP1-22 (P46FS4, gp5) * |
| TSP2 | gp55 TSP2-1 (ECML-4, gp190) | gp215 TSP2-1 (ECML-4, gp190) | gp171 TSP2-1 (ECML-4, gp190) | gp220 TSP2-5 (Bering, gp7) | gp138 TSP2-1 (SFP10, gp161) | gp1 TSP2-1 (SA157IW, gp3) |
| TSP3 | gp5 TSP3-1 (Moolton gp44) | gp216 TSP3-1 (Moolton, gp44) | gp172 TSP3-1 (Moolton, gp44) | gp219 TSP3-1 (Moolton, gp44) | gp137 TSP3-1 (Moolton, gp44) | ? |
| TSP4 | gp53 TSP4-12 (Maynard, gp38) | gp217 TSP4-2 (CBA120, gp213) | gp173 TSP4-9 (DET7, gp206) | gp218 TSP4-4 (Barely, gp5) | gp136 TSP4-9 (DET7, gp206) | gp2 TSP4-14 (AG3, gp213) |

* All proteins displayed high identity (>80%) to the TSP used for tail fiber typing by NCBI BLASTP with the exception of ChubbyThor gp208 identity to P46FS4 gp5 and gp1 identity to SA157IW gp3 which was only 70.46% over 74% of the protein and 35.79% over 26% of the protein, respectively. ? Indicates that we were unable to identify a TSP3 homolog for ChubbyThor.

4. Discussion

In this study, we report the further characterization of six phages isolated from local wastewater, and their relationship to a large section of the phages identified in the Vi01-like family (part of the ICTV *Ackermannviridae*). The other 144 fully sequenced and annotated *Enterobacteriaceae Ackermannviridae* available on NCBI have been discovered and isolated all over the world. Whole genome analysis of these 150 phages suggests five subclusters of *Enterobacteriaceae Ackermannviridae*, an increase of only one subcluster from a 2014 analysis of only 16 Vi01-like *Enterobacteriaceae Ackermannviridae*, suggesting high relatedness of these phages isolated from around the world. Herein one representative of each subcluster was studied to compare their genomic traits, similarities, and differences. The subclusters, simply titled A–E, were unsurprisingly found to be very similar superficially containing high protein conservation despite the weaker nucleotide conservation (Figures 1–3). The representatives from each subcluster had genomes of very similar length, between 157 and 164 kb in length, and each made up of approximately 200 genes. Their GC content was also within a very similar range, the largest difference being about 6%. On average the subclusters rested at about 60–70% average nucleotide similarity to one another.

Despite these differences the *Enterobacteriaceae Ackermannviridae* contain a core genome that was found to be 114 genes, mostly made up of DNA/RNA and structural proteins.

In total, the core 114 gene Vi01-like phage genome ranges between 55–67% of the size of the genomes of each phage in the cluster. That is, over half of the genome by gene count is conserved between each representative of each cluster. Clinker analysis also revealed a high amount of similarity in gene distribution (synteny) throughout the genome, with one notable area roughly 12.5 kb in length which clinker identified as dissimilar. This area was populated with genes that encode tail spike and tail fiber proteins, which has been previously reported to be highly variable in *Ackermannviridae*, facilitating broad host ranges among this phage family [49].

Approximately 50–60% of these genomes contained hypothetical proteins of unknown function. Using mass spectrometry, seven hypothetical proteins were validated through expressed spectra. Using Phyre analysis, putative functions were discovered that point to utilization of the hypothesized “ferrojan horse” method of cell entry, where a phage hides iron ions in its tail fibers to attach to the bacterial cell using already existing siderophore iron uptake pathways. However, preliminary investigation revealed that while Vi01-like phages may contain the ability to use this method of entry, it does not appear to be the phage’s main method of infection for the *Salmonella enterica* Typhimurium host investigated herein.

In host range analysis, the phages appeared to hew closely to the hosts in which they were discovered. All phages were able to infect *Salmonella* Typhimurium strains, including lab strains, iron uptake pathway mutant strains, and clinical CRE resistant strains. Of the other clinical strains, *Salmonella* Heidelberg showed phage infection in all tested phages other than FrontPhageNews, which may be due to its unique tail fiber TSP4-2 (see Table 9). These host range findings suggest these phages may be good candidates for *Salmonella* phage therapy and may aid in chimeric design for precise applications [110].

Supplementary Materials: The following supporting information can be downloaded at: <https://www.mdpi.com/article/10.3390/v16020289/s1>, Table S1: 150 Vi01-like *Enterobacteriaceae Ackermannviridae*; Table S2: Use of structural homology to identify putative functions of Vi01-like proteins. Table S3: Mass spectrometry of Sajous1 virions. Table S4. Strain information for *Salmonella*, *Shigella*, *Citrobacter* and *E. coli* clinical isolates utilized in this study.

Author Contributions: Conceptualization, J.H.G.; data curation, E.B.H. and J.H.G.; formal analysis, E.B.H. and J.H.G.; funding acquisition, J.H.G.; investigation, E.B.H., K.K.K.E., J.F., L.C.B., D.J. and M.M.; methodology, E.B.H. and J.H.G.; project administration, J.H.G.; resources, J.H.G.; software, S.T.; supervision, E.B.H. and J.H.G.; validation, E.B.H.; visualization, E.B.H.; writing—original draft, E.B.H., J.H.G., L.C.B. and D.J.; writing—review and editing, E.B.H. and J.H.G. All authors have read and agreed to the published version of the manuscript.

Funding: We are grateful for the generous support of the Department of Microbiology and Molecular Biology as well as the College of Life Sciences at Brigham Young University.

Institutional Review Board Statement: Not applicable.

Data Availability Statement: All supporting data is available in the Supplementary Material.

Acknowledgments: We thank the student authors of the genome announcement associated with the phages herein (Harris et al., 2023, [18]) for the initial discovery, isolation and characterization, including sequencing and annotation of these phages. We are grateful to Renee M. Tsois for the generous use of the *Salmonella enterica* serovar Typhimurium iron uptake mutants. We thank Michael Standing of the BYU Microscopy Lab for his aid with phage EM and Nathan Zuniga and the BYU Mass Spectrometry Facilities (BYU Department of Chemistry) for conducting the LC-MS-MS. We also thank Sherwood Casjens (University of Utah) as well as Graham Hatfull and the HHMI SEA PHAGES program for providing generous training in phage analysis.

Conflicts of Interest: The authors declare no conflict of interest.

References

1. Bergh, O.; Børsheim, K.Y.; Bratbak, G.; Heldal, M. High abundance of viruses found in aquatic environments. *Nature* **1989**, *340*, 467–468. [[CrossRef](#)] [[PubMed](#)]

2. Wommack, K.E.; Colwell, R.R. Virioplankton: Viruses in Aquatic Ecosystems. *Microbiol. Mol. Biol. Rev.* **2000**, *64*, 69–114. [[CrossRef](#)] [[PubMed](#)]
3. Hambly, E.; Suttle, A.C. The virosphere, diversity, and genetic exchange within phage communities. *Curr. Opin. Microbiol.* **2005**, *8*, 444–450. [[CrossRef](#)] [[PubMed](#)]
4. Grose, J.H.; Casjens, S.R. Understanding the enormous diversity of bacteriophages: The tailed phages that infect the bacterial family *Enterobacteriaceae*. *Virology* **2014**, *468–470*, 421–443. [[CrossRef](#)] [[PubMed](#)]
5. Chen, J.; Novick, R.P. Phage-Mediated Intergeneric Transfer of Toxin Genes. *Science* **2009**, *323*, 139–141. [[CrossRef](#)] [[PubMed](#)]
6. Schicklmaier, P.; Schmiegler, H. Frequency of generalized transducing phages in natural isolates of the *Salmonella typhimurium* complex. *Appl. Environ. Microbiol.* **1995**, *61*, 1637–1640. [[CrossRef](#)] [[PubMed](#)]
7. Boyd, E.F. Bacteriophage-encoded bacterial virulence factors and phage-pathogenicity island interactions. *Adv. Virus Res.* **2012**, *82*, 91–118.
8. Moghadam, M.T.; Amirmozafari, N.; Shariati, A.; Hallajzadeh, M.; Mirkalantari, S.; Khoshbayan, A.; Jazi, F.M. How Phages Overcome the Challenges of Drug Resistant Bacteria in Clinical Infections. *Infect. Drug Resist.* **2020**, *13*, 45–61. [[CrossRef](#)]
9. Carascal, M.B.; Cruz-Papa, D.M.D.; Remenyi, R.; Cruz, M.C.B.; Destura, R.V. Phage Revolution against Multidrug-Resistant Clinical Pathogens in Southeast Asia. *Front. Microbiol.* **2022**, *13*, 820572. [[CrossRef](#)]
10. Rahn, O. New Principles for the Classification of Bacteria. *Zentralblatt Bakteriologie. Parasitenkd. Infekt. Hyg.* **1937**, *96*, 273–286.
11. Toner, L.; Papa, N.; Aliyu, S.H.; Dev, H.; Lawrentschuk, N.; Al-Hayek, S. Extended-spectrum beta-lactamase-producing *Enterobacteriaceae* in hospital urinary tract infections: Incidence and antibiotic susceptibility profile over 9 years. *World J. Urol.* **2016**, *34*, 1031–1037. [[CrossRef](#)] [[PubMed](#)]
12. Reygaert, W.C. An overview of the antimicrobial resistance mechanisms of bacteria. *AIMS Microbiol.* **2018**, *4*, 482–501. [[CrossRef](#)] [[PubMed](#)]
13. Paterson, D.L. Resistance in Gram-Negative Bacteria: *Enterobacteriaceae*. *Am. J. Med.* **2006**, *119* (Suppl. 1), S20–S28; discussion S62–S70. [[CrossRef](#)] [[PubMed](#)]
14. Gupta, V.; Ye, G.; Olesky, M.; Lawrence, K.; Murray, J.; Yu, K. Trends in resistant *Enterobacteriaceae* and *Acinetobacter* species in hospitalized patients in the United States: 2013–2017. *BMC Infect. Dis.* **2019**, *19*, 742. [[CrossRef](#)]
15. Janda, J.M.; Abbott, S.L. The Changing Face of the Family *Enterobacteriaceae* (Order: “*Enterobacterales*”): New Members, Taxonomic Issues, Geographic Expansion, and New Diseases and Disease Syndromes. *Clin. Microbiol. Rev.* **2021**, *34*, e00174–20. [[CrossRef](#)] [[PubMed](#)]
16. Hooton, S.P.; Timms, A.R.; Rowsell, J.; Connerton, I.J. *Salmonella* Typhimurium-specific bacteriophage PhiSH19 and the origins of species specificity in the Vi01-like phage family. *Viol. J.* **2011**, *8*, 498. [[CrossRef](#)] [[PubMed](#)]
17. ICTV. Virus Taxonomy: 2020 Release. Available online: <https://ictv.global/taxonomy> (accessed on 28 December 2023).
18. Harris, E.B.; Anthony, L.B.; Ali, S.; Atkin, H.; Bowden, L.C.; Brugger, S.W.; Carr, E.L.; Eberhard, N.; Flor, S.; Gaertner, R.K.; et al. Complete genome sequences of five *Ackermannviridae* that infect *Enterobacteriaceae* hosts. *Microbiol. Resour. Announc.* **2024**, e0095023. [[CrossRef](#)]
19. Ugarriza, L.E.A.; Michalik-Provasek, J.; Newkirk, H.; Liu, M.; Gill, J.J.; Ramsey, J. Complete Genome Sequence of *Klebsiella pneumoniae* Myophage Magnus. *Microbiol. Resour. Announc.* **2019**, *8*, e01049–19.
20. Adriaenssens, E.M.; Van Vaerenbergh, J.; Vandenneuvel, D.; Dunon, V.; Ceysens, P.J.; De Proft, M.; Kropinski, A.M.; Noben, J.P.; Maes, M.; Lavigne, R. T4-related bacteriophage LIME stone isolates for the control of soft rot on potato caused by ‘*Dickeya solani*’. *PLoS ONE* **2012**, *7*, e33227. [[CrossRef](#)]
21. Akter, M.; Brown, N.; Clokie, M.; Yeasmin, M.; Tareq, T.M.; Baddam, R.; Azad, M.A.K.; Ghosh, A.N.; Ahmed, N.; Talukder, K.A. Prevalence of *Shigella boydii* in Bangladesh: Isolation and Characterization of a Rare Phage MK-13 That Can Robustly Identify Shigellosis Caused by *Shigella boydii* Type 1. *Front. Microbiol.* **2019**, *10*, 2461. [[CrossRef](#)]
22. Bai, J.; Jeon, B.; Ryu, S. Effective inhibition of *Salmonella* Typhimurium in fresh produce by a phage cocktail targeting multiple host receptors. *Food Microbiol.* **2019**, *77*, 52–60. [[CrossRef](#)]
23. Casjens, S.R.; Jacobs-Sera, D.; Hatfull, G.F.; Hendrix, R.W. Genome Sequence of *Salmonella enterica* Phage Det7. *Genome Announc.* **2015**, *3*, e00279–15. [[CrossRef](#)] [[PubMed](#)]
24. Chamblee, J.; Zeng, C.; O’Leary, C.J.; Gill, J.J.; Liu, M. Complete Genome Sequence of *Salmonella enterica* Serovar Enteritidis Myophage Mooltan. *Microbiol. Resour. Announc.* **2019**, *8*, e00187–19. [[CrossRef](#)] [[PubMed](#)]
25. Chen, L.; Guan, G.; Liu, Q.; Yuan, S.; Yan, T.; Tian, L.; Zhou, Y.; Zhao, Y.; Ma, Y.; Wei, T.; et al. Characterization and complete genomic analysis of two *Salmonella* phages, SenALZ1 and SenASZ3, new members of the genus Cba120virus. *Arch. Virol.* **2019**, *164*, 1475–1478. [[CrossRef](#)] [[PubMed](#)]
26. Duc, H.M.; Son, H.M.; Yi, H.P.S.; Sato, J.; Ngan, P.H.; Masuda, Y.; Honjoh, K.-I.; Miyamoto, T. Isolation, characterization and application of a polyvalent phage capable of controlling *Salmonella* and *Escherichia coli* O157:H7 in different food matrices. *Food Res. Int.* **2020**, *131*, 108977. [[CrossRef](#)] [[PubMed](#)]
27. Esmael, A.; Azab, E.; Gobouri, A.A.; Nasr-Eldin, M.A.; Moustafa, M.M.A.; Mohamed, S.A.; Badr, O.A.M.; Abdelatty, A.M. Isolation and Characterization of Two Lytic Bacteriophages Infecting a Multi-Drug Resistant *Salmonella* Typhimurium and Their Efficacy to Combat Salmonellosis in Ready-to-Use Foods. *Microorganisms* **2021**, *9*, 423. [[CrossRef](#)] [[PubMed](#)]
28. Fan, C.; Tie, D.; Sun, Y.; Jiang, J.; Huang, H.; Gong, Y.; Zhao, C. Characterization and Genomic Analysis of *Escherichia coli* O157:H7 Bacteriophage FEC14, a New Member of Genus Kuttervirus. *Curr. Microbiol.* **2021**, *78*, 159–166. [[CrossRef](#)] [[PubMed](#)]

29. Greenfield, J.; Shang, X.; Luo, H.; Zhou, Y.; Linden, S.B.; Heselpoth, R.D.; Leiman, P.G.; Nelson, D.C.; Herzberg, O. Structure and function of bacteriophage CBA120 ORF211 (TSP2), the determinant of phage specificity towards *E. coli* O157:H7. *Sci. Rep.* **2020**, *10*, 15402. [[CrossRef](#)]
30. Gutierrez, J.; Xie, Y.; Gill, J.J.; Liu, M. Complete Genome Sequence of *Salmonella enterica* Serovar Typhimurium Myophage Mutine. *Microbiol. Resour. Announc.* **2019**, *8*, e00401-19. [[CrossRef](#)]
31. Hsu, C.-R.; Lin, T.-L.; Pan, Y.-J.; Hsieh, P.-F.; Wang, J.-T. Isolation of a Bacteriophage Specific for a New Capsular Type of *Klebsiella pneumoniae* and Characterization of Its Polysaccharide Depolymerase. *PLoS ONE* **2013**, *8*, e70092. [[CrossRef](#)]
32. Islam, M.S.; Zhou, Y.; Liang, L.; Nime, I.; Yan, T.; Willias, S.P.; Mia, M.Z.; Bei, W.; Connerton, I.F.; Fischetti, V.A.; et al. Application of a Broad Range Lytic Phage LPST94 for Biological Control of *Salmonella* in Foods. *Microorganisms* **2020**, *8*, 247. [[CrossRef](#)] [[PubMed](#)]
33. Juliette, J.; Xie, Y.; Newkirk, H.; Liu, M.; Gill, J.J.; Ramsey, J. Complete Genome Sequence of *Salmonella enterica* Myophage Matapan. *Microbiol. Resour. Announc.* **2019**, *8*, e01017-19. [[CrossRef](#)] [[PubMed](#)]
34. Kabanova, A.P.; Shneider, M.M.; Korzhenkov, A.A.; Bugaeva, E.N.; Miroshnikov, K.K.; Zdorovenko, E.L.; Kulikov, E.E.; Toschakov, S.V.; Ignatov, A.N.; Knirel, Y.A.; et al. Host Specificity of the Dickeya Bacteriophage PP35 Is Directed by a Tail Spike Interaction with Bacterial O-Antigen, Enabling the Infection of Alternative Non-pathogenic Bacterial Host. *Front. Microbiol.* **2019**, *9*, 3288. [[CrossRef](#)] [[PubMed](#)]
35. Knecht, L.E.; Born, Y.; Pothier, J.F.; Loessner, M.J.; Fieseler, L. Complete Genome Sequences of *Erwinia amylovora* Phages vB_EamP-S2 and vB_EamM-Bue1. *Microbiol. Resour. Announc.* **2018**, *7*, e00891-18. [[CrossRef](#)]
36. Korf, I.H.E.; Meier-Kolthoff, J.P.; Adriaenssens, E.M.; Kropinski, A.M.; Nimtz, M.; Rohde, M.; van Raaij, M.J.; Wittmann, J. Still Something to Discover: Novel Insights into *Escherichia coli* Phage Diversity and Taxonomy. *Viruses* **2019**, *11*, 454. [[CrossRef](#)] [[PubMed](#)]
37. Kosznik-Kwaśnicka, K.; Ciemińska, K.; Grabski, M.; Grabowski, Ł.; Górniak, M.; Jurczak-Kurek, A.; Węgrzyn, G.; Węgrzyn, A. Characteristics of a Series of Three Bacteriophages Infecting *Salmonella enterica* Strains. *Int. J. Mol. Sci.* **2020**, *21*, 6152. [[CrossRef](#)]
38. Kwon, J.; Kim, S.G.; Kim, H.J.; Giri, S.S.; Bin Lee, S.; Park, S.C. Bacteriophage as an alternative to prevent reptile-associated *Salmonella* transmission. *Zoonoses Public Health* **2021**, *68*, 131–143. [[CrossRef](#)]
39. Matsushita, K.; Uchiyama, J.; Kato, S.I.; Ujihara, T.; Hoshiba, H.; Sugihara, S.; Muraoka, A.; Wakiguchi, H.; Matsuzaki, S. Morphological and genetic analysis of three bacteriophages of *Serratia marcescens* isolated from environmental water. *FEMS Microbiol. Lett.* **2009**, *291*, 201–208. [[CrossRef](#)]
40. Modi, R.; Hirvi, Y.; Hill, A.; Griffiths, M.W.; Heyse, S.; Hanna, L.F.; Woolston, J.; Sulakvelidze, A.; Charbonneau, D. Effect of Phage on Survival of *Salmonella* Enteritidis during Manufacture and Storage of Cheddar Cheese Made from Raw and Pasteurized Milk. *J. Food Prot.* **2001**, *64*, 927–933. [[CrossRef](#)]
41. Mutusamy, P.; Jothi, S.J.; Lee, S.Y.; Petersen, B.; Sicheritz-Ponten, T.; Clokie, M.R.J.; Loke, S.; Millard, A.; Parimannan, S.; Rajandas, H. Complete Genome Sequence of *Salmonella enterica* Bacteriophage PRF-SP1. *Microbiol. Resour. Announc.* **2021**, *10*, e0096521. [[CrossRef](#)]
42. Newase, S.; Kapadnis, B.P.; Shashidhar, R. Isolation and Genome Sequence Characterization of Bacteriophage vB_SalM_PM10, a Cba120virus, Concurrently Infecting *Salmonella enterica* Serovars Typhimurium, Typhi, and Enteritidis. *Curr. Microbiol.* **2019**, *76*, 86–94. [[CrossRef](#)] [[PubMed](#)]
43. Newkirk, H.N.; Lessor, L.; Gill, J.J.; Liu, M. Complete Genome Sequence of *Klebsiella pneumoniae* Myophage Menlow. *Microbiol. Resour. Announc.* **2019**, *8*, e00192-19. [[CrossRef](#)] [[PubMed](#)]
44. Park, M.; Lee, J.-H.; Shin, H.; Kim, M.; Choi, J.; Kang, D.-H.; Heu, S.; Ryu, S. Characterization and Comparative Genomic Analysis of a Novel Bacteriophage, SFP10, Simultaneously Inhibiting both *Salmonella enterica* and *Escherichia coli* O157:H7. *Appl. Environ. Microbiol.* **2012**, *78*, 58–69. [[CrossRef](#)] [[PubMed](#)]
45. Petrzik, K.; Vacek, J.; Brázdová, S.; Ševčík, R.; Koloniuk, I. Diversity of limestone bacteriophages infecting *Dickeya solani* isolated in the Czech Republic. *Arch. Virol.* **2021**, *166*, 1171–1175. [[CrossRef](#)] [[PubMed](#)]
46. Phohtaworn, P.; Supokaivanich, R.; Lim, J.; Klumpp, J.; Imam, M.; Kutter, E.; Galyov, E.E.; Dunne, M.; Korbsrisate, S. Development of a broad-spectrum *Salmonella* phage cocktail containing Viunalike and Jerseylike viruses isolated from Thailand. *Food Microbiol.* **2020**, *92*, 103586. [[CrossRef](#)] [[PubMed](#)]
47. Santiviago, C.A.; Blondel, C.J.; Quezada, C.P.; Silva, C.A.; Tobar, P.M.; Porwollik, S.; McClelland, M.; Andrews-Polymenis, H.L.; Toro, C.S.; Zaldivar, M.; et al. Spontaneous excision of the *Salmonella enterica* serovar Enteritidis-specific defective prophage-like element phiSE14. *J. Bacteriol.* **2010**, *192*, 2246–2254. [[CrossRef](#)] [[PubMed](#)]
48. Shahrababak, S.S.; Khodabandehlou, Z.; Shahverdi, A.R.; Skurnik, M.; Ackermann, H.-W.; Varjosalo, M.; Yazdi, M.T.; Sepehrizadeh, Z. Isolation, characterization and complete genome sequence of PhaxI: A phage of *Escherichia coli* O157:H7. *Microbiology* **2013**, *159* Pt 8, 1629–1638. [[CrossRef](#)]
49. Sørensen, A.N.; Woudstra, C.; Sørensen, M.C.H.; Brøndsted, L. Subtypes of tail spike proteins predicts the host range of Ackermannviridae phages. *Comput. Struct. Biotechnol. J.* **2021**, *19*, 4854–4867. [[CrossRef](#)]
50. Tatsch, C.O.; Wood, T.L.; Chamakura, K.R.; Everett, G.F.K. Complete Genome of *Salmonella enterica* Serovar Typhimurium Myophage Maynard. *Genome Announc.* **2013**, *1*, e00866-13. [[CrossRef](#)]

51. Thanh, N.C.; Nagayoshi, Y.; Fujino, Y.; Iiyama, K.; Furuya, N.; Hiromasa, Y.; Iwamoto, T.; Doi, K. Characterization and Genome Structure of Virulent Phage EspM4VN to Control *Enterobacter* sp. M4 Isolated From Plant Soft Rot. *Front. Microbiol.* **2020**, *11*, 885. [[CrossRef](#)]
52. Tian, C.; Zhao, J.; Zhang, Z.; Chen, X.; Wei, X.; Li, H.; Lin, W.; Ke, Y.; Hu, L.; Jiang, A.; et al. Identification and molecular characterization of *Serratia marcescens* phages vB_SmaA_2050H1 and vB_SmaM_2050HW. *Arch. Virol.* **2019**, *164*, 1085–1094. [[CrossRef](#)]
53. Xing, S.; Ma, T.; Zhang, X.; Huang, Y.; Mi, Z.; Sun, Q.; An, X.; Fan, H.; Wu, S.; Wei, L.; et al. First complete genome sequence of a virulent bacteriophage infecting the opportunistic pathogen *Serratia rubidaea*. *Arch. Virol.* **2017**, *162*, 2021–2028. [[CrossRef](#)]
54. Carstens, A.B.; Djurhuus, A.M.; Kot, W.; Jacobs-Sera, D.; Hatfull, G.F.; Hansen, L.H. Unlocking the Potential of 46 New Bacteriophages for Biocontrol of *Dickeya Solani*. *Viruses* **2018**, *10*, 621. [[CrossRef](#)] [[PubMed](#)]
55. Carter, C.D.; Parks, A.; Abuladze, T.; Li, M.; Woolston, J.; Magnone, J.; Senecal, A.; Kropinski, A.M.; Sulakvelidze, A. Bacteriophage cocktail significantly reduces *Escherichia coli* O157: H7 contamination of lettuce and beef, but does not protect against recontamination. *Bacteriophage* **2012**, *2*, 178–185. [[CrossRef](#)] [[PubMed](#)]
56. Chae, S.-J.; Kwon, T.; Lee, S.; Kang, Y.H.; Chung, G.T.; Kim, D.-W.; Lee, D.-Y. Genome Sequence of Bacteriophage GG32, Which Can Infect both *Salmonella enterica* Serovar Typhimurium and *Escherichia coli* O157:H7. *Genome Announc.* **2016**, *4*, e00802-16. [[CrossRef](#)] [[PubMed](#)]
57. Czajkowski, R.; Ozymko, Z.; Zwirowski, S.; Lojkowska, E. Complete genome sequence of a broad-host-range lytic *Dickeya* spp. bacteriophage φD5. *Arch. Virol.* **2014**, *159*, 3153–3155. [[CrossRef](#)] [[PubMed](#)]
58. Czajkowski, R.; Ozymko, Z.; Siwinska, J. The complete genome, structural proteome, comparative genomics and phylogenetic analysis of a broad host lytic bacteriophage varphiD3 infecting pectinolytic *Dickeya* spp. *Stand. Genomic Sci.* **2015**, *10*, 68. [[CrossRef](#)] [[PubMed](#)]
59. Day, A.; Ahn, J.; Fang, X.; Salmond, G.P.C. Environmental Bacteriophages of the Emerging Enterobacterial Phytopathogen, *Dickeya solani*, Show Genomic Conservation and Capacity for Horizontal Gene Transfer between Their Bacterial Hosts. *Front. Microbiol.* **2017**, *8*, 1654. [[CrossRef](#)] [[PubMed](#)]
60. Gencay, Y.E.; Gambino, M.; Prüssing, T.F.; Brøndsted, L. The genera of bacteriophages and their receptors are the major determinants of host range. *Environ. Microbiol.* **2019**, *21*, 2095–2111. [[CrossRef](#)] [[PubMed](#)]
61. Gendre, J.; Ansaldi, M.; Olivenza, D.R.; Denis, Y.; Casadesús, J.; Ginet, N. Genetic Mining of Newly Isolated Salmophages for Phage Therapy. *Int. J. Mol. Sci.* **2022**, *23*, 8917. [[CrossRef](#)]
62. Hooton, S.P.; Atterbury, R.J.; Connerton, I.F. Application of a bacteriophage cocktail to reduce *Salmonella* Typhimurium U288 contamination on pig skin. *Int. J. Food Microbiol.* **2011**, *151*, 157–163. [[CrossRef](#)] [[PubMed](#)]
63. Imklin, N.; Sriprasong, P.; Thanantong, N.; Lekcharoensuk, P.; Nasanit, R. Characterization and complete genome analysis of a novel *Escherichia* phage, vB_EcoM-RPN242. *Arch. Virol.* **2022**, *167*, 1675–1679. [[CrossRef](#)]
64. Xu, J.; Li, J.; Yan, Y.; Han, P.; Tong, Y.; Li, X. SW16-7, a Novel Ackermannviridae Bacteriophage with Highly Effective Lytic Activity Targets *Salmonella enterica* Serovar Weltevreden. *Microorganisms* **2023**, *11*, 2090. [[CrossRef](#)] [[PubMed](#)]
65. Liao, Y.-T.; Zhang, Y.; Salvador, A.; Ho, K.-J.; Cooley, M.B.; Wu, V.C.H. Characterization of polyvalent *Escherichia* phage Sa157lw for the biocontrol potential of *Salmonella* Typhimurium and *Escherichia coli* O157:H7 on contaminated mung bean seeds. *Front. Microbiol.* **2022**, *13*, 1053583. [[CrossRef](#)] [[PubMed](#)]
66. Kutter, E.M.; Skutt-Kakaria, K.; Blasdel, B.; El-Shibiny, A.; Castano, A.; Bryan, D.; Kropinski, A.M.; Villegas, A.; Ackermann, H.W.; Toribio, A.L.; et al. Characterization of a ViI-like phage specific to *Escherichia coli* O157:H7. *Virol. J.* **2011**, *8*, 430. [[CrossRef](#)]
67. Lagonenko, A.L.; Sadovskaya, O.; Valentovich, L.N.; Evtushenkov, A.N. Characterization of a new ViI-like *Erwinia amylovora* bacteriophage phiEa2809. *FEMS Microbiol. Lett.* **2015**, *362*, fmv031. [[CrossRef](#)] [[PubMed](#)]
68. Luna, A.J.; Wood, T.L.; Chamakura, K.R.; Everett, G.F.K. Complete Genome of *Salmonella enterica* Serovar Enteritidis Myophage Marshall. *Genome Announc.* **2013**, *1*, e00867-13. [[CrossRef](#)]
69. Matilla, M.A.; Salmond, G.P.C. Bacteriophage φMAM1, a Viunlikevirus, Is a Broad-Host-Range, High-Efficiency Generalized Transducer That Infects Environmental and Clinical Isolates of the Enterobacterial Genera *Serratia* and *Kluyvera*. *Appl. Environ. Microbiol.* **2014**, *80*, 6446–6457. [[CrossRef](#)]
70. Switt, A.I.M.; Bakker, H.C.D.; Vongkamjan, K.; Hoelzer, K.; Warnick, L.D.; Cummings, K.J.; Wiedmann, M. *Salmonella* bacteriophage diversity reflects host diversity on dairy farms. *Food Microbiol.* **2013**, *36*, 275–285. [[CrossRef](#)]
71. Nguyen, M.M.; Gil, J.; Brown, M.; Tondo, E.C.; de Aquino, N.S.M.; Eisenberg, M.; Erickson, S. Accurate and sensitive detection of *Salmonella* in foods by engineered bacteriophages. *Sci. Rep.* **2020**, *10*, 1746. [[CrossRef](#)]
72. Parmar, K.M.; Dafale, N.A.; Tikariha, H.; Purohit, H.J. Genomic characterization of key bacteriophages to formulate the potential biocontrol agent to combat enteric pathogenic bacteria. *Arch. Microbiol.* **2018**, *200*, 611–622. [[CrossRef](#)]
73. Pickard, D.; Toribio, A.L.; Petty, N.K.; van Tonder, A.; Yu, L.; Goulding, D.; Barrell, B.; Rance, R.; Harris, D.; Wetter, M.; et al. A Conserved Acetyl Esterase Domain Targets Diverse Bacteriophages to the Vi Capsular Receptor of *Salmonella enterica* Serovar Typhi. *J. Bacteriol.* **2010**, *192*, 5746–5754. [[CrossRef](#)] [[PubMed](#)]
74. Nguyen, K.T.; Bonasera, R.; Benson, G.; Hernandez-Morales, A.C.; Gill, J.J.; Liu, M. Complete Genome Sequence of *Klebsiella pneumoniae* Myophage May. *Microbiol. Resour. Announc.* **2019**, *8*, e00252-19. [[CrossRef](#)] [[PubMed](#)]
75. Soffer, N.; Abuladze, T.; Woolston, J.; Li, M.; Hanna, L.F.; Heyse, S.; Charbonneau, D.; Sulakvelidze, A. Bacteriophages safely reduce *Salmonella* contamination in pet food and raw pet food ingredients. *Bacteriophage* **2016**, *6*, e1220347. [[CrossRef](#)] [[PubMed](#)]

76. van Mierlo, J.; Hagens, S.; Witte, S.; Klamert, S.; van de Straat, L.; Fieseler, L. Complete Genome Sequences of Escherichia coli Phages vB_EcoM-EP75 and vB_EcoP-EP335. *Microbiol. Resour. Announc.* **2019**, *8*, e00078-19. [[CrossRef](#)] [[PubMed](#)]
77. Wu, J.-W.; Wang, J.-T.; Lin, T.-L.; Liu, Y.-Z.; Wu, L.-T.; Pan, Y.-J. Identification of three capsule depolymerases in a bacteriophage infecting *Klebsiella pneumoniae* capsular types K7, K20, and K27 and therapeutic application. *J. Biomed. Sci.* **2023**, *30*, 31. [[CrossRef](#)] [[PubMed](#)]
78. Zhang, J.; Hong, Y.; Fealey, M.; Singh, A.; Walton, K.; Martin, C.; Harman, N.; Mahlie, J.; Ebner, P. Physiological and Molecular Characterization of *Salmonella* Bacteriophages Previously Used in Phage Therapy. *J. Food Prot.* **2015**, *78*, 2143–2149. [[CrossRef](#)] [[PubMed](#)]
79. Broussard, K.; Xie, Y.; Newkirk, H.; Liu, M.; Gill, J.J.; Ramsey, J. Complete Genome Sequence of *Salmonella enterica* Siphophage Shelanagig. *Microbiol. Resour. Announc.* **2019**, *8*, e01033-19. [[CrossRef](#)]
80. Fong, S.A.; Drilling, A.J.; Ooi, M.L.; Paramasivan, S.; Finnie, J.W.; Morales, S.; Psaltis, A.J.; Vreugde, S.; Wormald, P.-J. Safety and efficacy of a bacteriophage cocktail in an in vivo model of *Pseudomonas aeruginosa* sinusitis. *Transl. Res.* **2019**, *206*, 41–56. [[CrossRef](#)]
81. Karpe, Y.A.; Kanade, G.D.; Pingale, K.D.; Arankalle, V.A.; Banerjee, K. Genomic characterization of *Salmonella* bacteriophages isolated from India. *Virus Genes* **2016**, *52*, 117–126. [[CrossRef](#)]
82. Liu, F.; Liao, Y.-T.; Li, R.W.; Wu, V.C.H. Complete Genome Sequence of Escherichia coli Phage vB_EcoM Sa1571w, Isolated from Surface Water Collected in Salinas, California. *Microbiol. Resour. Announc.* **2019**, *8*, e00718-19. [[CrossRef](#)]
83. Kearse, M.; Moir, R.; Wilson, A.; Stones-Havas, S.; Cheung, M.; Sturrock, S.; Buxton, S.; Cooper, A.; Markowitz, S.; Duran, C.; et al. Geneious Basic: An integrated and extendable desktop software platform for the organization and analysis of sequence data. *Bioinformatics* **2012**, *28*, 1647–1649. [[CrossRef](#)] [[PubMed](#)]
84. DNA Master. 2007. Available online: <http://cobamide2.bio.pitt.edu/computer.htm> (accessed on 28 December 2023).
85. Besemer, J.; Lomsadze, A.; Borodovsky, M. GeneMarkS: A self-training method for prediction of gene starts in microbial genomes. Implications for finding sequence motifs in regulatory regions. *Nucleic Acids Res.* **2001**, *29*, 2607–2618. [[CrossRef](#)]
86. Krumsiek, J.; Arnold, R.; Rattei, T. Gepard: A rapid and sensitive tool for creating dotplots on genome scale. *Bioinformatics* **2007**, *23*, 1026–1028. [[CrossRef](#)] [[PubMed](#)]
87. Tamura, K.; Stecher, G.; Kumar, S. MEGA11: Molecular Evolutionary Genetics Analysis Version 11. *Mol. Biol. Evol.* **2021**, *38*, 3022–3027. [[CrossRef](#)] [[PubMed](#)]
88. Whelan, S.; Goldman, N. A General Empirical Model of Protein Evolution Derived from Multiple Protein Families Using a Maximum-Likelihood Approach. *Mol. Biol. Evol.* **2001**, *18*, 691–699. [[CrossRef](#)] [[PubMed](#)]
89. Turner, D.; Reynolds, D.; Seto, D.; Mahadevan, P. CoreGenes3.5: A webserver for the determination of core genes from sets of viral and small bacterial genomes. *BMC Res. Notes* **2013**, *6*, 140. [[CrossRef](#)] [[PubMed](#)]
90. Gilchrist, C.L.M.; Chooi, Y.-H. clinker & clustermap.js: Automatic generation of gene cluster comparison figures. *Bioinformatics* **2021**, *37*, 2473–2475.
91. Page, A.J.; Cummins, C.A.; Hunt, M.; Wong, V.K.; Reuter, S.; Holden, M.T.G.; Fookes, M.; Falush, D.; Keane, J.A.; Parkhill, J. Roary: Rapid large-scale prokaryote pan genome analysis. *Bioinformatics* **2015**, *31*, 3691–3693. [[CrossRef](#)]
92. Jain, C.; Rodriguez-R, L.M.; Phillippy, A.M.; Konstantinidis, K.T.; Aluru, S. High throughput ANI analysis of 90K prokaryotic genomes reveals clear species boundaries. *Nat. Commun.* **2018**, *9*, 5114. [[CrossRef](#)]
93. Assafiri, O.; Song, A.A.-L.; Tan, G.H.; Hanish, I.; Hashim, A.M.; Yusoff, K. *Klebsiella* virus UPM2146 lyses multiple drug-resistant *Klebsiella pneumoniae* in vitro and in vivo. *PLoS ONE* **2021**, *16*, e0245354. [[CrossRef](#)] [[PubMed](#)]
94. Regue, M.; Fabregat, C.; Vinas, M. A generalized transducing bacteriophage for *Serratia marcescens*. *Res. Microbiol.* **1991**, *142*, 23–27. [[CrossRef](#)]
95. Schneider, C.A.; Rasband, W.S.; Eliceiri, K.W. NIH Image to ImageJ: 25 Years of image analysis. *Nat. Methods* **2012**, *9*, 671–675. [[CrossRef](#)] [[PubMed](#)]
96. Saitou, N.; Nei, M. The neighbor-joining method: A new method for reconstructing phylogenetic trees. *Mol. Biol. Evol.* **1987**, *4*, 406–425.
97. Zuckerkandl, E.; Pauling, L. Evolutionary Divergence and Convergence in Proteins. In *Evolving Genes and Proteins*; Academic Press: New York, NY, USA, 1965; pp. 97–166.
98. Stecher, G.; Tamura, K.; Kumar, S. Molecular Evolutionary Genetics Analysis (MEGA) for macOS. *Mol. Biol. Evol.* **2020**, *37*, 1237–1239. [[CrossRef](#)]
99. Felsenstein, J. Confidence Limits on Phylogenies: An Approach Using the Bootstrap. *Evolution* **1985**, *39*, 783–791. [[CrossRef](#)] [[PubMed](#)]
100. Mourosi, J.T.; Awe, A.; Guo, W.; Batra, H.; Ganesh, H.; Wu, X.; Zhu, J. Understanding Bacteriophage Tail Fiber Interaction with Host Surface Receptor: The Key “Blueprint” for Reprogramming Phage Host Range. *Int. J. Mol. Sci.* **2022**, *23*, 12146. [[CrossRef](#)]
101. Hatfull, G.F. Dark Matter of the Biosphere: The Amazing World of Bacteriophage Diversity. *J. Virol.* **2015**, *89*, 8107–8110. [[CrossRef](#)]
102. Kelley, L.A.; Mezulis, S.; Yates, C.M.; Wass, M.N.; Sternberg, M.J.E. The Phyre2 web portal for protein modeling, prediction and analysis. *Nat. Protoc.* **2015**, *10*, 845–858. [[CrossRef](#)]
103. Alcorlo, M.; Straume, D.; Lutkenhaus, J.; Hävarstein, L.S.; Hermoso, J.A. Structural Characterization of the Essential Cell Division Protein FtsE and Its Interaction with FtsX in *Streptococcus pneumoniae*. *mBio* **2020**, *11*. [[CrossRef](#)]
104. Yan, Y.; Moul, J. Detection of operons. *Proteins* **2006**, *64*, 615–628. [[CrossRef](#)]

105. Zulkower, V.; Rosser, S. DNA Features Viewer: A sequence annotation formatting and plotting library for Python. *Bioinformatics* **2020**, *36*, 4350–4352. [[CrossRef](#)]
106. Taboada, B.; Estrada, K.; Ciria, R.; Merino, E. Operon-mapper: A web server for precise operon identification in bacterial and archaeal genomes. *Bioinformatics* **2018**, *34*, 4118–4120. [[CrossRef](#)] [[PubMed](#)]
107. Bonnain, C.; Breitbart, M.; Buck, K.N. The Ferrojan Horse Hypothesis: Iron-Virus Interactions in the Ocean. *Front. Mar. Sci.* **2016**, *3*, 82. [[CrossRef](#)]
108. Tsois, R.M.; Bäumlér, A.J.; Heffron, F.; Stojiljkovic, I. Contribution of TonB- and Feo-mediated iron uptake to growth of *Salmonella typhimurium* in the mouse. *Infect. Immun.* **1996**, *64*, 4549–4556. [[CrossRef](#)] [[PubMed](#)]
109. Costa, L.F.; Mol, J.P.; Silva, A.P.C.; Macêdo, A.A.; Silva, T.M.; Alves, G.E.; Winter, S.; Winter, M.G.; Velazquez, E.M.; Byndloss, M.X.; et al. Iron acquisition pathways and colonization of the inflamed intestine by *Salmonella enterica* serovar Typhimurium. *Int. J. Med. Microbiol.* **2016**, *306*, 604–610. [[CrossRef](#)]
110. Gil, J.; Paulson, J.; Brown, M.; Zahn, H.; Nguyen, M.M.; Eisenberg, M.; Erickson, S. Tailoring the Host Range of *Ackermannviridae* Bacteriophages through Chimeric Tailspike Proteins. *Viruses* **2023**, *15*, 286. [[CrossRef](#)] [[PubMed](#)]
111. Plattner, M.; Shneider, M.M.; Arbatsky, N.P.; Shashkov, A.S.; Chizhov, A.O.; Nazarov, S.; Prokhorov, N.S.; Taylor, N.M.; Buth, S.A.; Gambino, M.; et al. Structure and Function of the Branched Receptor-Binding Complex of Bacteriophage CBA120. *J. Mol. Biol.* **2019**, *431*, 3718–3739. [[CrossRef](#)] [[PubMed](#)]

Disclaimer/Publisher’s Note: The statements, opinions and data contained in all publications are solely those of the individual author(s) and contributor(s) and not of MDPI and/or the editor(s). MDPI and/or the editor(s) disclaim responsibility for any injury to people or property resulting from any ideas, methods, instructions or products referred to in the content.